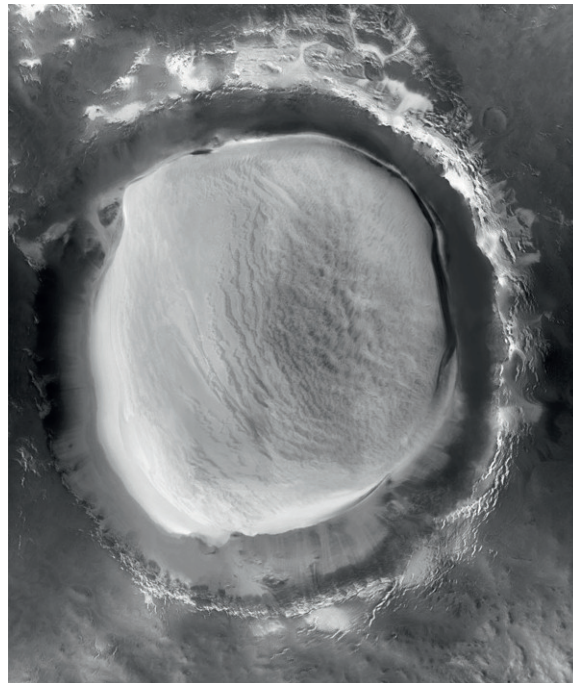


Ice Amount in Craters on the Martian Northern Polar Region



Angelique Bertilsson

MASTER OF SCIENCE PROGRAMME
Space Engineering

Luleå University of Technology
Department of Applied Physics and Mechanical Engineering
Division of Physics

Abstract

This Master Thesis is a work representing a scientific report, performed at the SETI institute and NASA Ames Research Center in collaboration with Luleå University of Technology.

The work consists of mapping craters on Mars northern polar region. The partly unexplored Martian northern hemisphere has like the southern hemisphere a great number of impacts all over the surface. Because of the Martian orbit and the tilt of the Martian axis, the impacts on the northern hemisphere are unexplored compared to those of the southern hemisphere.

The craters on the northern polar region are partly or totally covered by carbon dioxide frost and water frost during specific times in solar longitude. Separated from the northern residual polar cap, the craters on the northern polar region are believed to have residual ice during all Martian year. This ice is thought to be remnants of a former and greater polar cap consisting of water. As the perennial polar caps are related to the Martian climate history, the seasonal polar caps are related to the current climate and circulation. By understanding the sublimation and condensation of carbon dioxide and water, seasonal change and atmospheric circulation of current and future climate of Mars will be better known.

The craters have been analyzed with the help of context images and high resolution images, taken by the cameras CTX and HiRISE, riding on MRO.

All of the observed craters show different formations and depending on their location and how big they are, the covering of ice deposit varies. The main body of the craters observed within this work has appearance features within them. Unexplored features like Dark Dunes Spots, Dust Devils and Polygonal nets are just a few of them.

The ice covering a specific crater has been divided into different intervals in order to easier determine and analyze craters with summer ice. To investigate if the ice amount is due to different features observed within a crater, all observed features have been mapped and constitute a part of the results.

For future Martian scientific work, a description of every image of each specific crater has been stored within a database, together with an image.

Preface

This report has been written as a final step in acquiring a Master of Science degree of the Space Engineering Programme at Luleå University of Technology. The report represents the result of a collaboration between Luleå University of Technology, NASA Ames Research Center and the SETI Institution, in California.

The author would in particular thank Dr. Adrian Brown at the SETI institute for his time, knowledge, inspiration and enthusiasm for the Martian planet. Without his scientific experience and invaluable thoughts, this research work had taken much longer.

In addition, Dr. Chris P. McKay deserves a special thanks for initially presenting the idea of this scientific research of Mars, but also for the kind hospitality shown by him and his wife.

Further I will thank Prof. Sverker Fredriksson for giving the author this great opportunity, but also for carefully reading the text and giving constructive suggestions.

Thanks also to my friend and fellow worker, Mitra Hajigholi, for a scientific voyage of discovery of the Martian northern polar region.

Finally the author will warmly thank all people who have participated and made this work possible, and who also made this time an unforgettable experience. Special thanks to my family who have supported me with love and pushed me with cheerful calls. Also, I thank my lovely boyfriend who patiently has listened to my deep thoughts, while I was working with this project.

Kiruna, March 2010

Nomenclature

CRISM Compact Reconnaissance Imaging Spectrometer for Mars

CTX Context Camera

DDS Dark Dune Spot

HiRISE High Resolution Camera

MRO Mars Reconnaissance Orbiter

NPC Northern Polar Cap

NPLD North Polar Layered Deposit

NPR Northern Polar Region

NRIC Northern Residual Ice Cap

SPC Southern Polar Cap

List of Figures

2.1	The Mars Reconnaissance Orbiter, MRO	7
2.2	The HiRISE camera	8
2.3	The database	10
3.1	Phase diagram for water.	14
3.2	Water ice circulation model	15
4.1	Dune formation	18
4.2	Dune formation on Mars	18
4.3	Formation of dust devils	19
4.4	Defrosting on Mars	20
4.5	DDSs on Mars	22
4.6	The structure of polygonal nets	23
6.1	Ice amount in all observed craters	53
6.2	Relation between crater diameter, latitude and longitude	55
6.3	Relation between crater diameter and ice amount	57
6.4	Relation between craters containing dunes with the crater diameter	59
6.5	Relation between craters containing dunes and dust devils with the crater location	60
6.6	Relation between craters with no dunes but with dust devils as a function of solar longitude	61
6.7	Defrosting patterns appearance in solar longitude	62
6.8	DDSs upon and next to dunes	63
7.1	Formation of DDSs	70

List of Tables

1.1	Comparison of basic Mars data to the ones for Earth	4
6.1	Ice deposits within craters during the summer months.	58

Contents

1	Introduction	1
1.1	NASA Ames Research Center	1
1.2	The SETI Institute	2
1.3	Mars and the northern polar region	3
1.4	Outline of the thesis	5
2	Background	7
2.1	Mars Reconnaissance Orbiter	7
2.2	IAS viewer	9
2.3	Google Earth	9
2.4	The database	10
2.5	Criteria	11
3	How does ice behave on Mars?	13
3.1	Water ice	13
3.2	CO ₂ ice	15
4	What craters contain in the Martian northern polar region	17
4.1	Dunes	17
4.2	Dust devils	19
4.3	Defrosting features	20
4.4	Dark Dune Spots	22
4.5	Polygonal nets	23
5	Crater areology quality, related to seasonal ice coverage	25
5.1	Unnamed craters in latitudinal order	25
5.2	Named craters in alphabetic order	46
6	Results	53
6.1	Ice amount in all craters	53
6.2	Dunes	59
6.3	Dust Devils	59
6.4	Defrosting features	62
6.5	Dark dune spots	63
7	Conclusions and discussion	65
7.1	Ice amount in all craters	65
7.2	Dunes	66
7.3	Dust Devils	67
7.4	Defrosting features	68

7.5	Dark Dune Spots	69
7.6	Error sources	71
8	Future Work	73
	Vocabulary	75
	Appendix	83
	Attachment	91

Chapter 1

Introduction

1.1 NASA Ames Research Center

In the beginning of World War I in 1914 (Suckow, 2009), the Wright brothers were the first to make a powered airplane. In order for the United States to catch up, Congress founded in March 1915 (Suckow, 2009) an independent government agency, the National Advisory Committee for Aeronautics, NACA. Located in the heart of California's Silicon Valley, Moffett field, NACA created 1939 (Dino, 2008) an aircraft research laboratory, later known as Ames Research Center, ARC. In 1958 (Dino, 2008) ARC became a part of the National Aeronautics and Space Administration, NASA. After having founded a wind tunnel research on the aerodynamics of propeller-driven aircraft in 1956, Ames has expanded its role to research and technology in aeronautics and spaceflights.

Except for being a mission center for several NASA Science missions, like Lunar Crater Observations and Sensing Satellite, LCROSS, Kepler mission and Stratospheric Observatory for Infrared Astronomy, SOFIA, NASA Ames plays a big role in America's space and aeronautics programs.

NASA Ames also works collaboratively with the Federal Aviation Administration, FAA, an agency for transportation. Together they conduct research in air traffic management to make air travel safer, cheaper and more efficient. Like a reminder of its early aviation history, Moffett Field's Hangar One stands out as a recognizable landmark in the San Francisco Bay area. It was built in 1932 (Weselby, 2009) by the Navy to serve the West Coast base for the U.S. lighter-than-air aviation program. After Moffett Field in 1994 (Weselby, 2009) was decommissioned, the Navy transferred the hangar to NASA.

NASA Ames is also a leader in nanotechnology, supercomputing, fundamental space biology, biotechnology, aerospace and thermal protection system and humanfactors research. But as a research institution in astrobiology, NASA Ames focus on the effects of gravity on all living things, the nature and distribution of stars, planets and the possibility of life in the universe. In support of NASA missions, NASA Ames is also developing NASA Research Park, an integrated, dynamic research and education community created for different partnership with academia, non-profit organizations and industries.

1.2 The SETI Institute

The institute Search for Extra Terrestrial Intelligence, SETI, was founded as a private, nonprofit organization in 1984 (SETI, 2010c). SETI is a scientific and educational organization dedicated to scientific research, education and public outreach. Its mission is to understand, explain and explore the origin of the nature and the prevalence of intelligent life in the universe. It was after a published article in Nature in 1959 by two physicist at Cornell University, that led to the outstandingly suggestion that with help of radio telescopes detect the presence of extraterrestrial civilizations. At the same time in West Virginia, a young radio astronomer Frank Drake, created an experiment to search for signals from extraterrestrial intelligence. Drake spent two weeks sweeping his 26-meter radio telescope at the National Radio Astronomy Observatory, listening for extraterrestrial signals. It was the first SETI search, called Project Ozma. Since then SETI has done more than 98 projects around the world.

Today the SETI Institute consists of three major centers, divided into two areas, Research and Development, R&D, and Projects, whereof research is anchored by two centers: The center for SETI Research, where Jill Tarter and Bernard M. Oliver Chair are the leaders, the Carl Sagan Center for the Study of Life in the Universe directed by Frank Drake, and the center for Education and Public Outreach. The institution has today over 150 employed scientists, educators and support staff (SETI, 2010c) situated in Mountain View California (SETI, 2010b).

During 1994-2004, donations from individuals and grants from private foundations entirely funded the center for SETI Research at the SETI institute (SETI, 2010a). In 2005 an award were given by the NASA grant, for the work on signal detection for the Allen Telescope Array, an array of telescopes that together equals a 100-meter radio telescope. Still today, there are non governmental grants and donations that comprise the majority of the SETI Center funding.

Our understanding of life today is that, given a suitable environment at the right time and place, life will develop on other planets. Whether evolution will give rise to intelligence and build up technological civilizations is open to speculation. As such civilization could be detected across interstellar distances, SETI Research has together with UC Berkeley developed signal processing technology to search for signals from these technological civilizations in our galaxy.

SETI is a long-term project with possibilities of advanced technology to detect signals of intelligent civilizations.

"We believe we are conducting the most profound search in human history to know our beginnings and our place among the stars."(SETI, 2010c)

1.3 Mars and the northern polar region

Our red neighbour has been studied for centuries and even if the scientists have not found any life, the red, dusty planet, still gets our attention. Mars is the fourth planet from the Sun. Emitting a bright reddish-orange light, which reminded of the color of blood, Mars was first associated with war and therefore named after the Roman god of war (Steven, 2004). Today, the color reflects the surface composition of ironrich minerals in the soil, but also the chemical reactor between iron and oxygen, rust.

The Martian atmosphere is mainly composed of carbon dioxide and almost 100 times less dense than the atmosphere on Earth (Steven, 2004).

The tilt of the Martian axis is roughly 25° , compared with the Earth's 23.5° , which gives Mars almost the same seasons as on Earth. Due to gravitational forces from Jupiter and the other planets, the Earth's axis can vary between 22° and 25° . On Mars, those forces, especially the gravitational force from Jupiter, will affect even more. The Martian tilted axis can vary as much as 0° to 60° in timescales of hundreds of thousands to millions of years (Bennett et al., 2002). In addition, Earth has a moon that will help keep the Earth stabilized. Mars has no big moon. Instead it has two small moons, Phobos and Deimos, which are too small to give any stability to the planet's axis.

Another important effect is the shape on the Martian orbit. Compared to the Earth, Mars has a more elliptic orbit, which puts Mars significantly closer to the sun during the southern hemisphere summer, and further away during the southern hemisphere winter. This means that the southern Martian hemisphere seasons are much more extreme compared to the northern hemisphere. In addition to Keplers second law, where a planet orbiting a star moves faster in perihelion and slower when located in aphelion, the southern hemisphere summer is short and more intense compared to the northern hemisphere summer. During northern hemisphere summer, the planet will be located in aphelion and the northern hemisphere will be tilted towards the Sun, making its summer longer and milder. The same laws will give the southern hemisphere a long and colder winter compared to the northern hemisphere.

These extreme conditions cause a seasonal change in the Martian pressure and the carbon dioxide content in the atmosphere. In the northern hemisphere winter, the temperature will drop so much that the carbon dioxide will freeze out of the atmosphere as solid ice, which forms the north polar cap, NPC. At the same time, it is summer in the southern hemisphere and the rise in temperature will cause the frozen carbon dioxide in the polar cap to sublime.

Each winter, when the carbon dioxide freezes out of the atmosphere, the Martian poles remove a lot of gas from the atmosphere. Because of the sharp decrease of carbon dioxide the atmospheric pressure will change. As on Earth, Mars pressure also changes due to daily weather changing.

Giving these extremes, it could be expected to see that all carbon dioxide in the south polar cap, SPC, would be sublimated into carbon dioxide gas during the southern hemisphere summer. However, this is not the case. Instead, the carbon

CHAPTER 1. INTRODUCTION

dioxide in the SPC will remain frozen throughout the southern summer and remaining Martian year.

Many observed images of Mars show evidence of liquid water that once have flown on the surface. Today, no liquid water can exist on the surface without vaporizing, because of Mars low atmospheric pressure.

At first glance, Mars seems to be an unlikely place for life. But as on Earth, life has a remarkable potential to evolve in the most extreme environments. So there is a possibility when looking closer beneath the surface that liquid water might exist and provide a habitable zone for existing life.

Table 1.1: Comparison of basic Mars data to the ones for Earth

	Earth	Mars
Average distance from the Sun	1 AU (149.6 million km)	1.52 AU (227.9 million km)
Orbital period (yr)	1	1.881
Orbital inclination	0.00°	1.85°
Orbital eccentricity	0.017	0.093
Axis tilt	23.45°	23.98°
Equatorial Radius	6378 km	3397 km
Mass (rel. Earth)	1 ($5.97 \cdot 10^{24}$ kg)	0.107 ($6.42 \cdot 10^{23}$ kg)
Rotation period	23 h 56 min	24 h 37 min
Surface gravity (rel. Earth)	1	0.38
Atmospheric composition	78% N ₂ , 21% O ₂ , 0.9% Ar	95% CO ₂ , 2.7% N ₂ , 1.6% Ar
Average surface temperature	15 °C	-53 °C
Average surface pressure	1.013 bar	0.005 bar

The northern hemisphere is relatively flat and young compared to the heavily cratered and older southern hemisphere (Smith et al., 1998). The NPR consists of flat plains that surround the Planum Boreum, a slightly circular plateau with a diameter of 1.1 to 1.2 km (Tanaka and Scott, 1987). The impact craters on the northern plains are few and the elevation seems to be below the average Martian surface level (Bennett et al., 2002). In the view of Mars early history, during the heavy bombardment, the Martian surface is expected to have impact craters all over the surface. That is not what is observed today and the impact craters on the northern plains are suggested to have been erased or covered since then (Bennett et al., 2002). Compared with the southern hemisphere, the northern plains show evidence of lava flows, suggesting that liquid lava have covered the old impact craters. In some regions in the northern hemisphere, faint craters can be seen, suggesting that the lava flows was not thick enough to cover all craters completely. This confirms that the Martian surface was once covered by impact craters all. By study these old impact craters clues of Mars evolution can be found.

Most likely Mars has had a warmer climate than today. Existing water has then frozen as the planet got colder. A kilometer-thick dome of dusty water ice covers the North Polar Layered Deposits, NPLD, covering the Planum Boreum today. With the help of radar transparency it is known that the polar layered deposit, PLD, are predominantly composed of water ice with less than 10 percent dust (Byrne, 2009). These remnants of icy rich layers provide information from the

past 10^5 to 10^9 years Byrne (2009) of the Martian climate. Each layer is thought to provide that specific climate information from when the layer was deposited. The NPLD then might represent records of how the Martian climate has changed in recent past. The north residual ice cap, NRIC which partially cover the PLD, is mainly composed of water ice. By observing the visible albedo of the ice, the RIC is suggested to be contaminated with dust or large ice grains. In some extent the Residual Ice Cap, RIC, appears to be currently stable. However, some reversible changes in time scales of one to two Martian years, have been observed (Byrne, 2009). The RIC probably provides information of Mars annual variability of the current climate. Older deposits, probably situated beneath the PLDs, might reflect a different Martian climate than present. Each winter, when the carbon dioxide freezes out of the atmosphere, the NPLD will be covered by seasonal carbon dioxide frost, extending the cap. This seasonal cap only last for a fraction of the Martian year.

1.4 Outline of the thesis

The thesis describes the craters on the Martian northern polar region, with the help of images taken by CTX and HiRISE. The thesis will, with an analyzing description give a view of how water and carbon dioxide ice amount change within the craters depending on season and location. The work describes the craters from the author's perspective and what kind of features have been observed within the craters.

Chapter 2 introduces the reader to the basic information about one of the satellites orbiting Mars and its instruments, used for this work. Also, a short description of useful software and where they can be found is given. In Chapter 2.5 the criteria utilized for this study of work are listed.

Chapter 3 covers characteristics of how water ice and carbon dioxide ice behaves, compared to the Earth.

Chapter 4 contains descriptions of features which have been observed within the craters throughout the work. The given features, will be used when describing the characteristics of all observed craters. Basic information of where they are observed and how they can be recognized are given, together with how they are believed to appear.

Chapter 5 describes all the observed and studied craters on the Martian northern hemisphere. Description of the craters areology, its location, its observed features and how the water and carbon dioxide ice vary with time will be taken up. All the studied images for respective crater, can be found in appendix.

Chapter 6 describes all the results made from the images taken of the craters and their features.

Chapter 7 contains conclusions and thoughts of the results in Chapter 6 together with sources of error that can give entailment and affect the results.

Chapter 2

Background

2.1 Mars Reconnaissance Orbiter

Mars Reconnaissance Orbit, MRO, is a multipurpose satellite with a new spacecraft design provided by Lockheed Martin Space Systems. Also, it is the first satellite that has been designed from ground up for aerobraking. It means that the friction from the Martian atmosphere is used to slow down the speed and create the shape of the orbit around the planet (Baerg et al., 2010c). Compared with previous spacecrafts, MRO is designed to be smarter, more reliable, more agile and more productive.



Figure 2.1: Mars Reconnaissance Orbiter, MRO has orbited around Mars since 2005, giving a lot of scientific images of the Martian surface.

Source: <http://solarsystem.nasa.gov/multimedia/gallery/PIA04918-browse.jpg>

Retrieved:2010-02-11

Previous Mars missions have shown that water have flowed on the surface of Mars. But it still remains a mystery whether water was ever around long enough to provide habitat for life. MRO's primary mission is to search for evidence that water has persisted for a long period on the Martian surface. Orbiting around Mars,

MRO will investigate three different purposes; global mapping, regional surveying and target specific spots on the surface in high resolution (Baerg et al., 2010b). During its mission MRO will perform eight different science investigations at Mars.

At launch, the spacecraft did not weight more than 2.180 kg, and all instruments and subsystems had a weigh less than 1.031 kg (Baerg et al., 2010c). MRO was launched in August 2005, and its primary mission will end in December 2010, about five-and-a-half years after launch.

There are six scientific instruments, three engineering instruments and two more science-facility experiments onboard on MRO. Three cameras and one spectrometer have been used for this work, whereof two of the cameras, CTX and HiRISE together with the spectrometer CRISM.



Figure 2.2: HiRISE, a high resolution camera capable to provide detailed images of 0.25 meter per pixel. Source: http://marsoweb.nas.nasa.gov/HiRISE/images/hirise_flight_structure.jpg Retrieved:2010-03-11

The CTX camera

CTX is a context camera designed to obtain grayscale images and provide a wider context for data collected by the HiRISE camera and the mineral-finding spectrometer, CRISM. The camera has a resolution of 6 meter per pixel and a swath width of 30 km at an altitude of 290 km (Malin et al., 2007). The camera observes features, e.g., candidate landing sites, and conducts a scientific investigation of the Martian geomorphic, geologic and meteorological processes (Malin et al., 2007). Compared with other cameras riding on MRO, CTX provides images of larger areas of the Martian terrain.

The HiRISE camera

High Resolution Imaging Science Experiment, HiRISE, is a high resolution camera that commenced operations in 2006. The camera is a 0.5 reflecting telescope, which gives a colored (red, green and IR) and detailed resolution of 0.25 meter per pixel (McEwen et al., 2007). In contrast to the CTX camera, the HiRISE camera takes smaller images in higher resolution, providing images with greater details of the Martian surface than has previously been achieved.

The HiRISE camera is also called “The People’s Camera” as the unprecedented access of images shortly after they have been received and processed are at the

disposal for the general public.

With help of HiRISE, better studies and understanding of volcanic landforms, channels, valleys and other features that can be seen on the Martian surface, can be reached.

The spectrometer on MRO

Compact Reconnaissance Imaging Spectrometers for Mars, CRISM, is a spectrometer used for searching residual minerals that have been formed early in the Martian history. From an altitude of 300 km (Baerg et al., 2010a) CRISM operates in the visible and in the infrared regions of light (362 nm to 3920 nm) and map regions on the Martian surface in scales of 18 meter across.

To measure the amount of light reflected at different wavelengths from the Martian surface, CRISM uses a different kind of spectroscopy called reflectance spectroscopy, which focus on the reflected radiation from different materials. To detect certain mineral patterns or past water, colors reflected by the sunlight breaks down to a wide spectrum, which helps CRISM to determine the mineralogy of the surface (Beisser, 2010).

2.2 IAS viewer

The Image Access Solutions, IAS Viewer, is a relatively new program, providing great potential for easier handling large images efficiently. IAS Viewer is a free software application to view images in JPEG2000, JP2 format.

The software is available for Linux, Mac OSX and Windows and allows the user to zoom, pan, select different bands, modify and open multiple images.

Since the full resolution HiRISE images are stored in the JP2 format, the IAS Viewer software has been used throughout the work for observing both HiRISE and CTX images.

The IAS Viewer can be downloaded from the HiRISE homepage:
<http://hirise.lpl.arizona.edu/jp2.php>

2.3 Google Earth

Google Earth is a free, virtual globe software, created to show a 3D version of planet Earth and its moon, but also, in the latest version, Mars. From the beginning the program was called EarthViewer 3D and created by Keyhole Inc., a company acquired by Google. The software was in 2005 released as Google Earth and compatible with, among others, Windows 2000, XP, Vista, 7, Mac OSX, iPhoneOS and Linux.

With Google Earth, showing detailed satellite images of terrain and buildings, you can go wherever you want to, on both the Earth and the Mars, explore the stars and galaxies in the sky and the deep seas on Earth. With the help of Google

CHAPTER 2. BACKGROUND

Earth with Mars, craters on the Martian NPR have been mapped and their diameters have been measured. The software has been a tool for searching after special craters and places on the surface of Mars.

Google Earth can be downloaded from the Google homepage:
<http://earth.google.com/>

2.4 The database

To store information about the craters from the Martian NPR and to easier handle all de images from different craters, a database has been created, *Information of craters on the Martian Northern Polar Region*.

The Database have been created with Microsoft Office Access 2007. It stores all the basic information of the mapped craters poleward from 60° latitude, on the Martian NPR. Also, the image-ID and information about the HiRISE and CTX images that cover the craters are stored, i.e., what kind of camera that has been used, when the image was acquisitioned, at what Earth time the image was taken and at what Martian season in solar longitude that the time corresponds to.

Information on Craters in the Martian Northern Polar Region
Luleå University of Technology 2010
Created by Angelique Bertilsson
Information added by Angelique Bertilsson and Mitra Hajigholi

Name of Area or the Crater: Lomonosov Crater
Center Latitude: 64.95°
Center Longitude (East): 350.80°
Acquisition Date: 27 February 2008
Crater ID: A01 Lomonosov Crater
Image ID: PSP_007440_2455
Image Location (North and East): 65.0°N 351.0°E
Camera: HiRISE
Solar Longitude (Degrees): 37.6°
Solar Longitude (Season): Northern Spring
Diameter of the Crater (average km): 112
How much ice does the Crater Contain: 50
Website: http://hriase.lpl.arizona.edu/PSP_007440_2455

Features: Black features
Mitra Notes:
Angelique Notes: HiRISE: Small part in the middle of the crater. Defrosting patterns are visible. Black features are seen to appear. CRISM: small area in the middle part, completely covered by water ice.

Run Query

Figure 2.3: All information of the craters are stored in a database, created with help of Microsoft Office Access 2007.

Information about the craters location in latitude and longitude and how much ice the craters contain is described. Even the craters rough diameters are included, determined using a measuring tool in the Google Earth software. The measuring of ice amount in the craters is divided into four major parts depending on how much ice that covers the crater; the crater contains no ice, the crater contains less than 50 percent ice, the crater contains more than 50 percent ice and the crater is full of ice. In this work no consideration of the ice depth is taken, nor how deep the craters are.

Also, the database store information if the crater contains different features like polygonal nets, defrosting, dust devils, dunes and/or DDSs, and where the images of the crater can be downloaded.

2.5 Criteria

There are many images taken by both CTX and HiRISE over different seasons, to monitor the change of the ice amount within the craters. During this work 500 images of craters on the NPR have been examined and monitored. The images are taken over all Martian seasons, 0° - 360° , graded in solar longitude, L_s .

Sometimes, the Sun will be in a position, relative to the camera, where it will glare the camera and deteriorate the images. Also, a cloud or a dust storm could obscure the crater, and the ice amount, if present, will not be seen. Because no good scientific observation and no adequate good description of the ice cover can be made with these images, they are disregarded. Craters have then been selected poleward from 60° latitude with the following criteria utilized:

- The crater should be clearly visible in all studied images and easily identified, i.e., no clouds or dust storms obscure the crater area.
- The craters should have a rough diameter of more than 10 km unless the crater has a formal name.

Chapter 3

How does ice behave on Mars?

3.1 Water ice

The importance of water for life has been known since long. Mars is in many ways similar to Earth, and if water exists, life might too. So far, research has shown that water exists in the Martian residual ice caps, at shallow depth in the regolith, on the surface and in the atmosphere. Still, there are major unresolved questions involving the exchange of water between the north and the south polar reservoirs, e.g., how much water there is and what kind of time scales are involved (Titus et al., 2008).

Due to the low Martian atmospheric pressure, 5.6 mbar, water is only present either as frost, ice or as vapor. As Figure 3.1 shows, pure liquid water may only exist at temperatures above 273.16 K (0.01°C) in correlation with a pressure above 6.12 mbar (611.73 Pa). According to Figure 3.1, it is then impossible for water to exist in liquid form on the Martian surface.

The North Polar Region, NPR, shows repeated patterns from year to year of forming water-ice clouds. The water ice will cover the residual ice cap as a seasonal ice cap. These clouds of water ice can be widened as far south as 48° N and obscure the residual cap as early as $\sim 167^\circ$ in solar longitude (Titus et al., 2008). Water ice clouds have also been observed near the equator. If the temperature at night gets low enough, clouds of water-ice can be created (Calvin, 2008).

With consistent values over two Martian northern summers, a peak of atmospheric water vapor was viewed in the north at $L_s \sim 120^\circ$ with MGS-TES, Mars Global Surveyor -Thermal Emission Spectrometer, by Calvin (2008). In contrast, the water over the southern cap is observed to be highly variable. This implies that a water cap underlies the residual carbon dioxide ice in the south, with a highly variable history of exposure and sublimation (Titus et al., 2008).

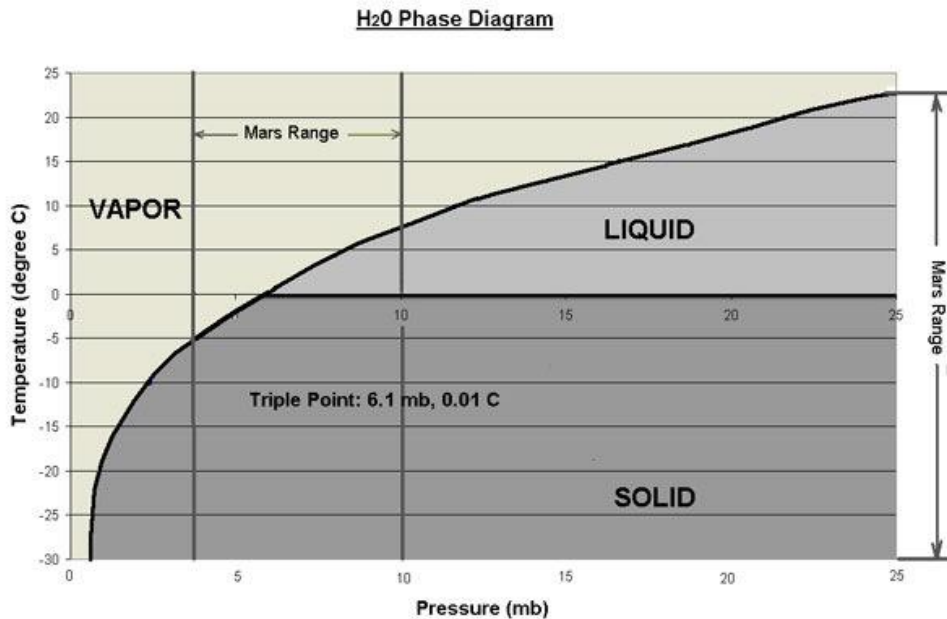


Figure 3.1: At typical Martian temperatures and pressure, liquid water is not stable. For liquid water to exist on the Martian surface the atmospheric pressure need to be between 6.1 mb and 10 mb in a temperature range of $+0.1^{\circ}\text{C}$ to $+9^{\circ}\text{C}$.

Source: [http://lh3.ggpht.com/_tXIBMJ6p7yE/SbmMtB8p-xI/AAAAAAAAAKY/wbWOSdPd7Vk/s1600-h/H2O-Phase-Diagram\[4\].jpg](http://lh3.ggpht.com/_tXIBMJ6p7yE/SbmMtB8p-xI/AAAAAAAAAKY/wbWOSdPd7Vk/s1600-h/H2O-Phase-Diagram[4].jpg). Retrieved: 2010-03-21

The average water ice/frost precipitation in the north is $100\text{ }\mu\text{m}$, compared to $50\text{ }\mu\text{m}$ in the south. Models suggest that the amount of water sublimated from the northern residual cap is insufficient to account for the peak amounts in the atmosphere, and that the regolith exchange must also contribute to the observed atmospheric reservoir in the northern summer (Titus et al., 2008).

The Mars Odyssey Gamma Ray Spectrometer/Neutron Spectrometer, GRS/NS, shows large amounts of subsurface ice in both the north and the south reservoirs, mid- to high-latitude ice-permeated ground. The fact that the southern hemisphere lacks a large water-vapor peak means that the ground ice in the southern hemisphere is not in exchange with the atmosphere and may therefore be more deeply buried, which is consistent with the thermal inertia data (Titus et al., 2008).

The polar caps have the role of a summertime source and a wintertime sink for water. The seasonal variations of the atmospheric water content may depend on the exchange with the regolith (Jakosky and Haberle, 1992).

To better understand the water cycle on Mars, especially the role of clouds, general Circulation Models are created and used, as the one in Figure 3.2 (Titus et al., 2008).

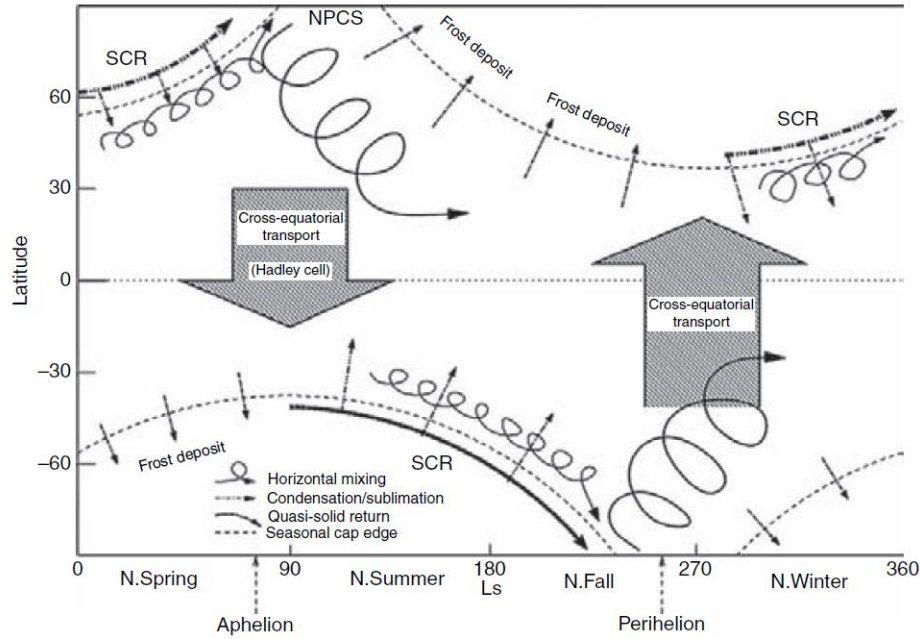


Figure 3.2: The components of the water cycle, including the migration of water ice along of the retreating seasonal caps. SCR: Seasonal Cap Retreat, NPCS: North Polar Cap Sublimation (Titus et al., 2008).

3.2 CO₂ ice

The Martian atmosphere is composed of mainly carbon dioxide. Because of the shape of the Martian orbit, which is more elliptic than Earth, Mars will come closer to the sun during its southern hemisphere summer and farther away during southern hemisphere winter. Hence the Martian seasons are much more extreme compared to the seasons on Earth. These extremes will cause seasonal changes in the pressure and carbon dioxide content of the atmosphere. As carbon dioxide needs five times the atmospheric pressure on Earth at sea level to become liquid and since the atmospheric pressure on Mars is even lower, the carbon dioxide on Mars will go directly from solid ice to gas (Russell, 2009).

Carbon dioxide ice, also referred to as dry ice, is a non-polar molecule with a zero dipole moment. It then has a low thermal and electrical conductivity where intermolecular van der Waals forces act.

In the northern Martian hemisphere the temperature will drop so much that the carbon dioxide will freeze out of the atmosphere as solid ice, adding a coating of dry ice to the polar caps. In the mean time the southern hemisphere has summer, and the frozen carbon dioxide in the polar cap sublimates into carbon dioxide gas. As the southern summer ends and the northern summer begins, the whole process reverses. Overall there will be roughly 25 percent of the atmosphere (Titus et al., 2008), were 95 percent is carbon dioxide that will cycle seasonally between the northern and the southern polar caps annually. The carbon dioxide cycle dominates the atmospheric circulation. It is this process which drives the current

CHAPTER 3. HOW DOES ICE BEHAVE ON MARS?

Martian climate, where carbon dioxide freezes out of the atmosphere in autumn and winter and then sublimates back into the atmosphere in the spring.

With an ambient Martian pressure of 6 mbar, carbon dioxide and water ice will sublime/condense at a temperature of 150 K and 200 K (Xie et al., 2007), respectively (Russell, 2009). Since carbon dioxide is more volatile than water, the surface at low temperatures, when carbon dioxide frost is present, will act like an efficient cold trap for water.

Observing carbon dioxide and water ice in images, the reflectance of fresh carbon dioxide and water ice is similar to each other, which makes them difficult to distinguish in monochrome or multiband reflectance imaging unless coverage extends longward of about 1 μm . All frozen carbon dioxide will sublime during the northern summer leaving a residual polar cap, made of water ice mixed with Martian dust, which will last throughout the summer. Compared with the southern hemisphere the frozen carbon dioxide will retain frozen throughout the Martian year.

Small amounts of water or dust will have a large effect on the reflectance as pure carbon dioxide has a low absorption coefficient, e.g., the reflectance will be 25 percent less with 0.1 percent fine dust or 1 percent water in a region of 1.5 - 2.5 μm bands (Titus et al., 2008). In visible wavelengths only dust can darken carbon dioxide. Looking with thermal IR, even the grain size of carbon dioxide will have an important rule on emissivity. Also, the changing of albedo can tell the size of the carbon dioxide grains. Seasonal frost with grain size less than 100 μm will be brighter than permanent ice with grain size about 1 mm in mid summer. But according to the work of James et al. (2005) pure carbon dioxide is bright with small variations in wavelength in the visible part of the spectrum. Visible albedo then weakly depends on the grain size of pure carbon dioxide. However, the emissivity of the surface carbon dioxide deposits and the wavelength dependent albedo control the process of deposition and sublimation in the Martian caps.

The knowledge of the seasonal polar cap and the understanding of condensation and sublimation of carbon dioxide and water will allow us to understand recent, current and future Martian climate. Craters located at the seasonal polar cap regions, provide a great opportunity, especially those with high albedo deposits of frost and/or ice, to study condensation and sublimation of water and carbon dioxide. It is therefore important to understand how carbon dioxide ice changes and interact with the Martian surface and atmosphere and explore the craters located in the NPR.

Chapter 4

What craters contain in the Martian northern polar region

4.1 Dunes

In geosystems a dune is defined as a hill of sand that has been created by aeolian processes. Formed by interactions with the winds, the dunes have different shapes and sizes. Based on the various types of their shape and how the dunes are formed they are categorized differently. By observing the changing patterns of the sand dunes, a better understanding of the interaction between the Martian surface and the atmosphere can be made. By observing the dune activity the Martian winds can be determined, but also how and at what rate the Martian wind moves the sediment around.

Sand grains move with the wind in two distinct ways, either by surface creep or by saltation, where saltation is the primary method (Mangimeli, 2010). As the wind picks up the sand grains from the surface, it will give them a forward momentum. Depending on the weight of the grains they will be carried away by the wind over different distances. Bigger grains will fall to the ground after a short distance. If the surface is composed of coarse grains, the sand grains will bounce up in the air and the wind will, again, provide the grain a forward momentum, while lighter grains will be moved by the wind to longer distances. When lighter grains then strikes the sandy surface they will more likely bury themselves and the impact will eject a second grain into the air (Mangimeli, 2010). As the winds picks up the grains it will lose its force and velocity. Also, a small pile of sand can decrease the velocity and the strength of the wind and cause even more sand to be deposited. This will eventually create a large pile of sand, defined as a dune. However, since the gravitational force is three times weaker on Mars than on Earth, the sand grains will not be pushed downward by the gravity in the same way as they do on Earth. They will therefore be able to stay in the air much longer before they strike the surface.

CHAPTER 4. WHAT CRATERS CONTAIN IN THE MARTIAN NORTHERN POLAR REGION



Figure 4.1: The wind will continue to move the sand up to the top and create a pile of sand. When the pile becomes too steep, it will collapse under its own weight. When the right steepness is reached the dune will be stable. Depending on the properties of the material, the angle of the steepness will be different (Mangimeli, 2010).

Source: <http://www.nature.nps.gov/geology/usgsnps/dune/dunefmtn1.gif> Retrived:2010-02-15

Martian dunes were discovered in 1972 by Mariner 9 (Baerg et al., 2010d) and are today actively studied.

A major part of the observed craters on the Martian NPR contains dunes. These dunes are most likely located in the center or in the middle part of the crater. Also, if the crater contains a central peak, some craters observed contain dunes that are located on or behind the central peak. Some craters also have dunes located on the surface around them, outside the crater rim.

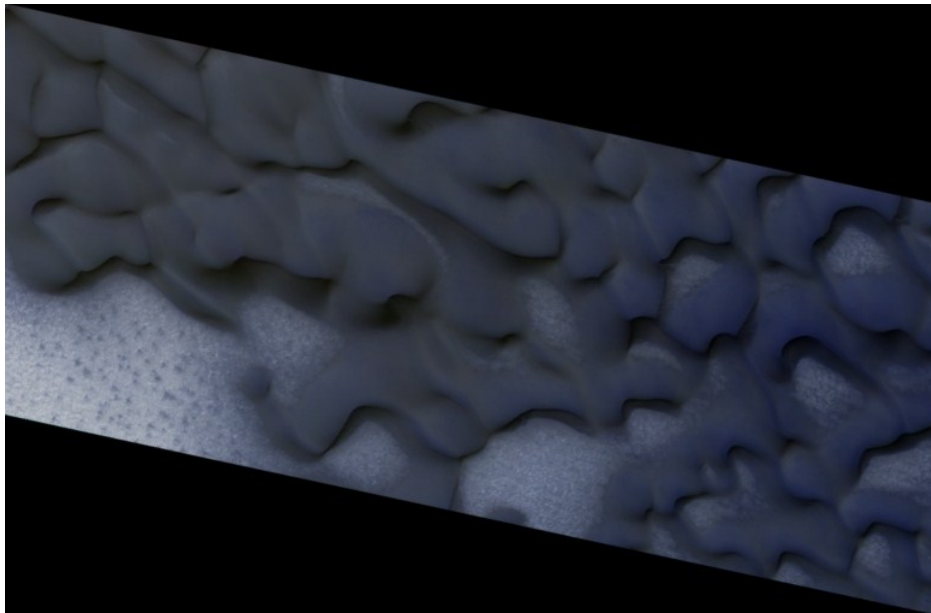


Figure 4.2: Image PSP_009087_2550, is taken by the HiRISE camera and shows a dune formation in the middle of a crater at latitude 74°.

4.2 Dust devils

Dust devils are leaving tracks of dark lines, on the Martian surface, suggested to be effective for raising dust in the low-density atmosphere. Dust devils are described as convective vortices made by dust and sand, emerging from high rotating wind speeds, significant electrostatic fields and reduced pressure (Balme and Greeley, 2006).

On both Mars and Earth, dust devils are a common atmospheric phenomenon. On Mars, dust devils have been observed by the Mars Pathfinder, by the MGS camera and by both Viking orbiters and landers (Ferri et al., 2003). On Earth, dust devils can be observed in the terrestrial dry lands and desert landscapes.

Dust devils are characterized by upward moving and spiraling flows, which are caused by insulation that is heating up the near-surface air. When the ground is heated by the sun, warm air will raise and interact with the surrounding wind. The air will move towards the center of the updraft to spin, while attempting to conserve angular momentum. The friction of the surface will then reduce the angular momentum of the spinning air and disturb the balance between the centrifugal and pressure gradient forces (Ferri et al., 2003). When the centrifugal forces decrease, the warm, nearsurface air will converge toward the center of the vortex. In turn, the concentration of the ambient vorticity will increase by the radial inflow. If dust is captured in the rising vortex, a dust devil will appear.

By moving over nearby areas of hot air, the dust devils are able to sustain themselves longer. When the dust devil enters a terrain where the surface temperature is lower, cooler air will be sucked in and disturb the balance and the dust devil will dissipate in seconds.

According to the work of Renno et al. (2000), the typical temperature difference and pressure within the dust devils vary between 4 and 8 K and from 2.5 to 4.5 hPa.

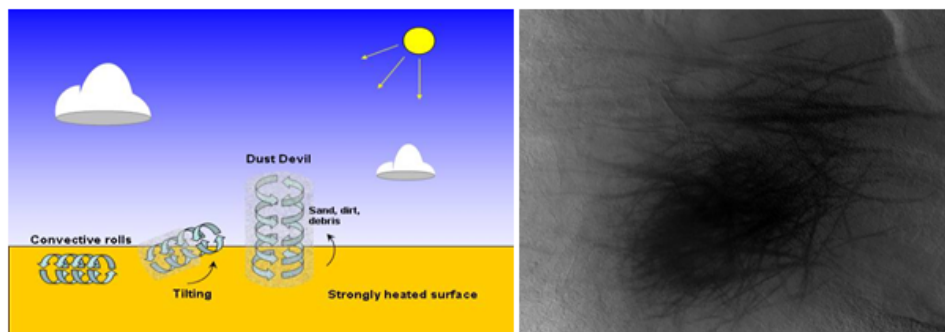


Figure 4.3: In the left image. Dust devils are created through a mechanism, different from those behind tornados. When the sun heats up the dry surface, the air starts to produce convective rolls. Some of these rolls get tilted upright, producing a dust devil. When dust and debris get caught inside the vortex, the dust devil will be visible. To the right, the image, PSP_010241_2485, is taken with the HiRISE camera at $L_s = 138.5^\circ$, northern summer. clear tracks of dust devils can be observed in the middle of a high latitude crater, 68.4° N and 189.3° E.

Source: http://www.weatherquestions.com/dust_devil.jpg. Retrieved:2010-02-15

4.3 Defrosting features

As the Martian spring season begins, the atmospheric and surface temperature will gradually start to increase. Carbon dioxide ice has a lower sublimation point than water ice, so it will begin to sublimate back into the atmosphere and expose the water ice or regolith below. As the temperature increases it will become warm enough for the water ice to sublimate to the atmosphere. On average, the temperature in the NPR increases until the middle of the summer. This process is called defrosting. As defrosting occurs interesting patterns and features can be observed.

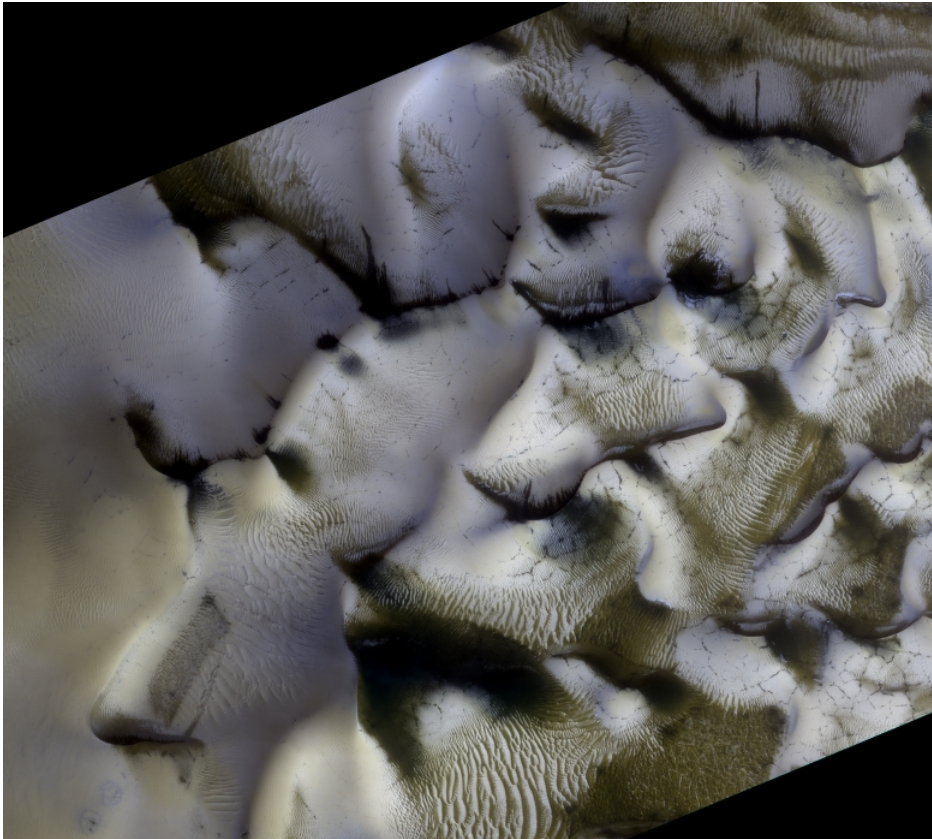


Figure 4.4: Image PSP_007805_2505, is taken by the HiRISE camera, and shows defrosting patterns on the dunes in the middle of the Louth crater. Sublimating water and carbon dioxide frost gives a shape of stripes or waves that appear darker than the area surrounding it.

By observing the albedo of the ice/frost within the craters and monitoring the seasonal change during one Martian year, defrosting features can be discovered. The regolith in the crater floor has a low albedo and ice a high albedo, in particular carbon dioxide ice as compared with water ice. An increase in albedo is most likely due to condensation of ice onto the crater floor/wall. A decrease in albedo could be due to defrosting of the area, but also due to the fact that ice can age, or as a result of very usual dust storms occurring in the NPR periodically.

Aged ice gives lower albedo as a result of its larger ice/frost grain size. A larger

4.3. DEFROSTING FEATURES

amount of small ice grains will have more surfaces to reflect the incoming light, compared to the larger ones. During the dust storm season, large amounts of dust from the large dune fields in the NPR will cover the ice/frost deposit. When dust settles on ice, it will decrease its albedo significantly.

Another way of observing defrosting features in images is by searching for the patterns that remind of defrosting patterns occurring on Earth. When ice/snow/frost melt it starts to move. Movement of ice can give the shape of stripes or waves that appear darker than the area surrounding it. The ice melts most likely only during the day when sunlight heats up the surface, and freezes during the night. The melting process is much slower on Mars than on Earth. So, as the ice melts and freezes during day and night, patterns of ice layers can be observed. Generally the defrosting patterns start to appear on the rim (the location that gains most sunlight during the day, and has the highest incline). Then is defrost on the crater wall and finally on the floor (which is usually deep and covered by the crater walls shadow).

4.4 Dark Dune Spots

Throughout this work Dark Dune Spots (DDSs) seem to form only in craters containing dunes, and when defrosting patterns occur. In rare cases DDSs can be observed even when there is no defrosting. These dark albedo features can be located upon and next to dune formations on the flat ground, which usually have at least a thin ice or frost layer covering them. DDSs seem to be formed under these ice sheets, unexposed to the atmosphere. The first signs when DDSs start to form are similar to spots, being a few meters in diameter. Under these sheets of ice the spots develop by increasing radially in size until they become exposed to the atmosphere.

Compared to the surrounding area the features appear to be dark/black. With time and increasing thermal heat they increase in number and grow in size. Depending on where the spots appear they will develop differently. If they appear on top of a dune peak they will stream down similar to how a liquid streams downhill, looking like streaks featuring the same albedo as the spots.

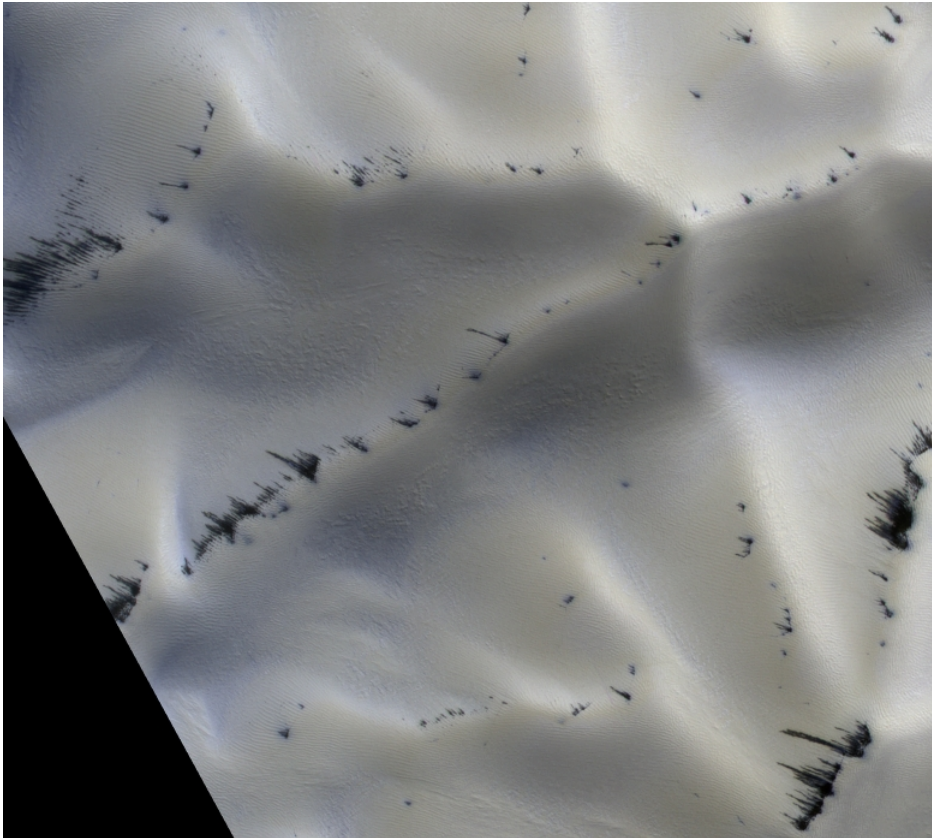


Figure 4.5: Image PSP_08131_2615, is taken by the HiRISE camera and shows the structure of dark albedo features in the Jojutla crater. Appearing on top of a dune peak they will stream down similar to how a liquid streams downhill, looking like streaks.

4.5 Polygonal nets

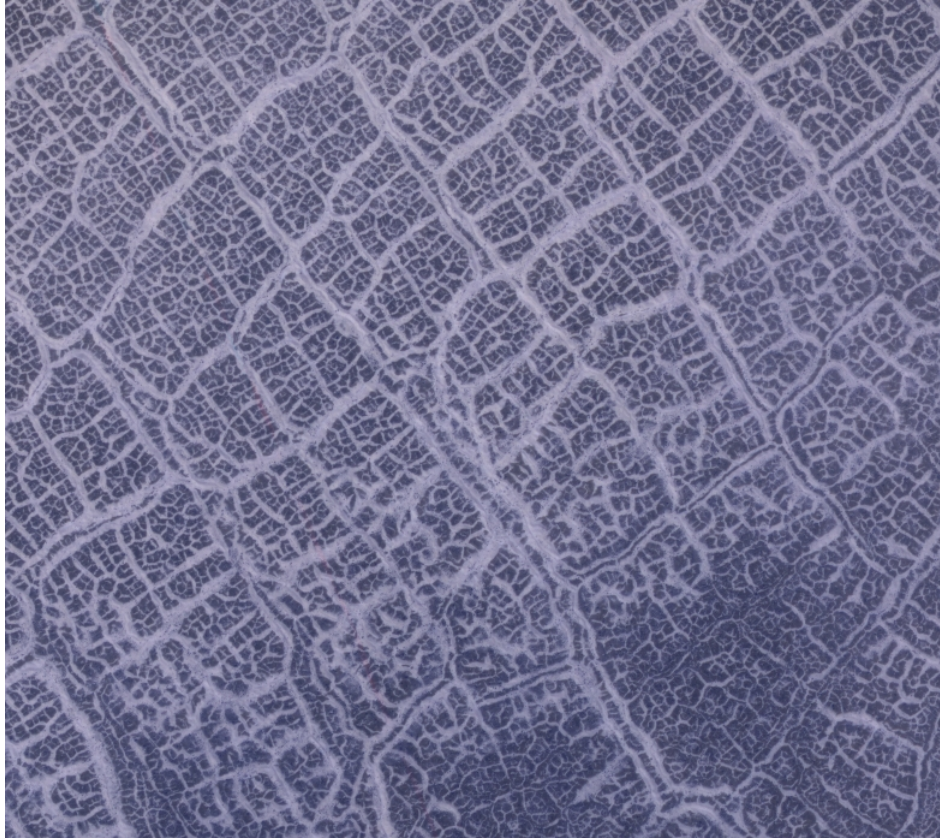


Figure 4.6: Image PSP_007571_2490 is taken by the HiRISE camera and shows the structure of polygonal nets in a mid-latitude crater.

In some craters, a structure of polygonal nets can be observed on the crater floor. The nets can be compared with small raised walls that together constitute a structure of polygons. These small ridges are, in late spring, observed to sometimes have ice on the tops, which makes the structure more distinct to the surrounded crater floor. The structure can be seen on the crater floor, on the crater wall, and both on and beside a central peak within the crater.

CHAPTER 4. WHAT CRATERS CONTAIN IN THE MARTIAN NORTHERN POLAR REGION

Chapter 5

Crater areology quality, related to seasonal ice coverage

5.1 Unnamed craters in latitudinal order

Crater: 60N_148E

Location: 60.43°N, 147.72°E

Three images are taken over a polar crater, during the middle of the northern spring, reaching from 41.57° to 58.85° in solar longitude. The crater has a lot of ice during this time. However, the middle part is almost ice free. Some ice is still left in small hollowed out areas within the polygonal structure, which covers the middle region of the crater. In the latest image, the ice is still covering larger parts of the east and southern regions of the crater, the crater walls and the crater rim. Dust devils can be observed in the middle of the crater, where the surface is uncovered.

Crater: 60N_129E

Location: 60.36°N, 129.37°E

All of the images are taken by the CTX camera, starting from the middle of the northern spring and reaching to the middle of northern summer, from 44.81° to 140.42° in solar longitude. There are five images covering the roughly 24 km large crater. In these images, almost no change can be seen. The crater is almost uncovered except for some ice on the eastern crater wall and on the crater rim. Structures of polygonal nets are visible in the middle region of the crater. Black tracks of dust devils are visible behind and across the crater.

CHAPTER 5. CRATER ARELOGY QUALITY, RELATED TO SEASONAL ICE COVERAGE

Crater: 60N_101E

Location: 60.40°N, 101.25°E

The roughly 21 km sized crater is located close to an area called Alba Fossae. This complex crater, with a peak in the middle, is covered by three images, two taken by CTX and one by HiRISE, during the northern spring and summer, at 58.27°, 68.6° and 128.7° in solar longitude. Images show that the crater has a polygonal shaped ground. Defrosting patterns are visible during late northern spring, and thinner layers of ice are observed in the whole crater. However, earlier in spring the crater has an ice/frost layer covering almost the whole crater.

Crater: 60N_222E

Location: 60.12°N, 221.9°E

The almost 16 km wide crater is localized in the Vastitas Borealis area. Three out of four images covering the crater are taken by CTX and one by HiRISE. The images are all taken during the northern spring season, 20.29° to 60.56° in solar longitude, and all show a cloudy area partly obscuring the dunes in the center of the crater. East crater wall and rim has a thin ice layer that decreases fairly rapidly with time. Tracks of dust devils are visible at $L_s = 60.56^\circ$.

Crater: 60N_313E

Location: 60.32°N, 313.47°E

In the region called Vastitas Borealis the roughly 20 km in diameter crater is located. Three CTX images cover the crater during $L_s = 44.11^\circ - 100.63^\circ$. A very thin layer of ice is observed on the crater wall in the earliest image. The regolith is observed to have polygonal patterns over wave formed hills and a peak in the middle of the crater. A couple of gullies are observed on the north-east crater wall. At the end of the spring, defrosting patterns appears on the northern crater wall. Dust devil tracks are visible in the southern part of the crater close to the dunes, which increase in numbers during the beginning of summer. With increasing solar longitude the dunes become darker, and almost all ice sublimates.

Crater: 60N_281E

Location: 60.15°N, 280.83°E

The crater is located in the Vastitas region, and is roughly 37 km in diameter. The three CTX and two HiRISE images cover the crater over $L_s = 51^\circ - 141.7^\circ$. The crater has several gullies formed on its rim, small dune formations at the bottom of the crater next to its large peak, and a small crater inside. There is a thin ice layer covering the whole crater during the middle of the spring. The dunes become darker with solar longitude, and dark dust is spread north by the wind. Also, some of the gullies, north-west of the crater, are observed to become darker in albedo.

Crater: 60N_251E

Location: 60.25°N, 251.08°E

The almost 22 km crater is a complex one. There is only one CTX image in total covering the crater, showing a peak and a crater floor with polygonal nets. This image covers the whole crater during middle of the northern spring at $L_s = 58.27^\circ$. No signature of an ice cover is observable, but tracks of dust devils on the eastern side of the crater floor are observed.

Crater: 61N_90E

Location: 60.59°N, 89.66°E

There are ten images taken of the almost 21 km wide crater, located in the southern part in the northern hemisphere. The images are taken from the beginning of the northern spring and reaching to the middle of the northern summer, 28.59° to 142.01° in solar longitude.

From the western crater rim gully formations are visible. Some vague structures of polygonal nets are visible in the middle of the crater. Also, some dunes are located in the north-western part of the crater. In the end of the spring and in the beginning of the summer, dust devils appear around the dunes. Some small amount of ice is visible on the eastern crater rim in the beginning of the spring. Except for that, the crater is more or less empty in all images taken during the spring and summer.

Crater: 61N_88E

Location: 60.65°N, 87.74°E

The CTX camera has taken five images of the 61 km large crater, located in the southern part of the NPR. The images are taken during the northern spring and reaching to the middle of the northern summer, 36.09° to 147.19° in solar longitude. The crater floor in the middle of the crater is composed of raised ridges, and some vague structure of polygonal nets is visible as well. The crater has almost no ice during this period. From the middle of the spring, to the latest image, in the summer, dust devils are visible around the dunes in the middle of the crater.

Crater: 61N_229E

Location: 61.46°N, 229.45°E

One CTX image covers the almost 22 km crater, located north-west in the Vastitas Borealis region, at $L_s = 68.63^\circ$. The very rough terrain on the crater bottom shows spots of ice layering in hollowed areas. A thicker ice layer is observed at the north-east rim with darker spots visible.

CHAPTER 5. CRATER ARELOGY QUALITY, RELATED TO SEASONAL ICE COVERAGE

Crater: 61N_22E

Location: 61.31°N, 21.51°E

The roughly 13 km wide crater is located in the southern region of the northern hemisphere. Two images are taken by the CTX camera during the northern spring, 47.98° and 69.79° in solar longitude. On the earlier images, a small amount of ice is observable. Some of this ice is located on the inner side of the north-eastern crater rim, which becomes even smaller in later images. Some ice is located in small hollowed areas on the crater floor, which is composed of a polygonal structure.

Crater: 61N_312E

Location: 61.19°N, 311.61°E

The almost 30 km crater, covered by three images, is located at Vastitas Borealis. Two CTX images and one HiRISE image cover the crater between $L_s = 41.4^\circ$ and 63.59° . Both images show almost no ice, except in hollowed out areas at the peak region and on the crater rim. Some high peaks of the large dune formation at the bottom of the crater show some ice deposit. Data observations from CRISM during this time period do not show any water or carbon dioxide ice deposit.

Crater: 61N_308E

Location: 61.35°N, 307.7°E

The roughly 22 km crater is located in the Vastitas Borealis. It has two CTX and two HiRISE images covering the crater in total between $L_s = 20.6^\circ$ and 43.7° . The crater is observed to have several gullies around the entire crater rim, which are partly covered by a thin ice layer. A large field of dark dunes is visible at the bottom of the crater. Early in the spring, a small part in the south-east of the crater has a thin ice layer.

Crater: 62N_6E

Location: 61.7°N, 6.36°E

The crater is located in an area called Acidalia Planitia, south of the NPR. There are three images taken by CTX during the northern hemisphere spring, reaching from solar longitude 41.29° to 68.46° . In the middle of the roughly 24 km large crater, dunes are observable, but also a structure of polygonal nets can be observed on the crater floor. The crater is almost completely empty of ice at this period. Some ice is still left and can be observed on the edge of the crater rim, in the east of the crater image.

Crater: 62N_222E

Location: 62.41°N, 221.76°E

The crater is located in an area called Scandia Colles. The almost 16 km crater is covered by two images both during middle of the northern spring. The crater shows a thin ice layer on its western rim and wall. However, in the north of the crater, a thick ice layer is visible on top of the unusual hills created on the crater rim. Other features visible are tracks of dust devils in the middle of the crater.

Crater: 63N_12E

Location: 63.4°N, 11.92°E

The crater is located in the southern part of the NPR. There are three images taken over the roughly 41 km large crater, whereof two are taken by the CTX camera and one by the HiRISE camera. All of the images are taken during the northern spring, reaching from 29.16° to 64° solar longitude. Some kind of plateau formation can be seen in the middle of the crater. Also a structure of polygonal nets can be seen around this plateau on the crater floor. A couple of dunes are located in the north-east of the crater. The crater is almost empty of ice at this period. However, the dunes are still covered and some DDSs have appeared on the tops. Some of the ice can also be seen in small hollowed out areas on the crater floor. Aside from this, the only ice observed is the one located around the crater, on the crater rim.

Crater: 63N_187E

Location: 62.53°N, 186.81°E

In the area called Vastitas Borealis, the almost 35 km wide crater is located. Nine images cover the crater from the middle of the spring to the middle of summer.

In the beginning of the northern spring the crater is observed to have a thin ice layer on part of its rim and on its peak, which are surrounded by dunes. With time, more ice accumulates on the peak, and, consequently in the end of the spring the peak has a thick ice layer covering it. The ice cover increases in area, reaching and surrounding the dunes next to the peak as well. However, the ice on its rim decreases with time.

At summer the dunes in the crater become dark, and tracks of dust devils are visible during middle and late summer. The rugged crater floor shows no sign of ice, but small valleys in the center of the crater do. Also, the crater peak has a thin ice layer in the end of the summer.

Crater: 63N_292E

Location: 63.46°N, 292.48°E

The roughly 17 km crater is covered by seven images (four CTX and three HiRISE images). At 37.2° in solar longitude, the crater barely shows any sign of ice, as most is on the rim. Its many gully formations, which are a proof of water flowing down the crater, are partly ice covered by a thin layer. The large dunes in the bottom of this crater are also partly covered by a thin ice layer at this time. During the beginning of summer, the dunes have become much darker as all the ice has sublimed. Tracks of dust devils are observed to cross the dunes and the crater floor. Still there can be observed a thin layer of ice on the eastern crater rim.

CHAPTER 5. CRATER ARELOGY QUALITY, RELATED TO SEASONAL ICE COVERAGE

Crater: 63N_296E

Location: 63.49°N, 295.87°E

The 21 km wide crater is located in the region called Vastitas Borealis. Four images in total cover the crater during $L_s = 22.11^\circ - 62.26^\circ$. The CTX image taken during early spring shows, that some dunes are ice covered even though the crater is partly obscured by clouds. During the middle of spring the crater has a frost or a thin ice layer covering its walls and hollowed areas at the bottom of the crater. The dunes seem to no longer have any ice coverage and have therefore become dark in color. Odd frost features are observed around the crater, as stripes going straight from the rim and out. Fainter dust devil tracks are visible, crossing the crater, which become stronger in pattern during the end of the spring.

Crater: 64N_132E

Location: 63.53°N, 131.82°E

With a diameter of almost 25 km, the crater is located in the southern part of the northern hemisphere. Three images are taken, whereof one in high resolution. All of the images are taken during the northern spring, from 22.33° to 45.26° in solar longitude. In the earliest image, ice can be seen in depths on the crater floor and around, on the crater wall. Also, structures of polygonal nets are visible in the middle of the crater floor. In the latest image, almost all the ice has sublimed, and the only ice left are small stripes on the crater rim.

Crater: 64N_31E

Location: 64°N, 31°E

The almost 21 km big, low-latitude crater has only one image covering it. It is taken by the CTX camera during middle of the northern spring, 48.58° in solar longitude. In this image a structure of polygonal nets is visible on the crater floor. Only small amount of ice is visible as small stripes on the crater rim. Except for that, the crater is empty of ice.

Crater: 64N_234E

Location: 64.26°N, 233.73°E

The almost 14 km crater is located in the area Vastitas Borealis. Only one image, taken by CTX, covers the crater during the northern spring at $L_s = 41.92^\circ$. At this time the crater is covered by a very thin ice/frost layer on partial areas on the crater floor, but also on the rim. Fainter tracks of dust devils are visible in this simple crater, which does not show any peak.

Crater: 65N_284E

Location: 65.31°N, 283.85°E

Above an area called Tantalus Fossae, the roughly 22 km crater is located. Three CTX images, during the northern spring, and one HiRISE image, during the northern summer, cover the crater in total between $L_s = 15.83^\circ$ and 128.7° . In the

earliest image by CTX, the crater is partly obscured by water ice clouds. Yet it can be observed that the dunes are all completely ice covered on the large peak and next to a large field of very strange features (looking like cracks filled with ice). DDSs are also clearly visible on the dunes. However, the rest of the crater has a very thin ice layer, which shows defrosting patterns. The images during the middle of the spring show that the dunes have emerged from the ice cover, and the rest of the peak has an even thicker ice layer than before. Spots of ice are also visible on the rim and inside hollows on the eastern crater wall.

Crater: 65N_330E

Location: 65.37°N, 329.58°E

The almost 18 km crater is located in the area Vastitas Borealis. Four CTX and two HiRISE images cover the crater between 20.14° to 176.1° in solar longitude. In the earliest image the crater has a thin ice layer covering almost the whole crater. Polygonal nets have valleys filled with ice on the crater floor, and the dunes clearly visible on the bottom of the crater are covered by a thin ice layer. However, defrosting patterns are visible and DDSs have emerged and prospered over all the dune formations. Thicker ice layers are observed on the eastern side of the crater and at the top of the rim.

During the middle of the spring most of the ice has sublimated and the dunes are dark and uncovered by ice. Still the eastern crater wall, next to the dunes, is covered by a thicker ice layer compared with the rest of the crater, which is observed during the summer as well. Streaks of ice can be seen, all around the crater, from the rim and down to the bottom of the crater. When the summer season comes, the crater gets hit by a dust storm. All over the crater, inside and outside the crater, tracks of dust devils can be observed in images taken during the middle of the northern summer.

Crater: 65N_339E

Location: 65.36°N, 338.77°E

The roughly 21 km crater is located in the Vastitas Borealis region. The crater is covered by three CTX images in total, covering its seasonal behavior between $L_s = 33.9^\circ$ and 144.75° .

In the earliest image, the crater is obscured by clouds, although by observing the albedo difference, the southern and western part of the crater seem to have a thicker ice layer compared with the surrounding area. Partly ice covered dunes are also visible. Later during the middle of spring the crater is observed to have a thin ice layer covering the southern rim. The regolith seems to have a cracking pattern at the bottom of the crater, next to the dunes. A small crater is observed north-west of the bottom of the crater.

During the middle of spring the crater shows no sign of water. The dune formation has become dark and tracks from dust devils are visible. Another small crater is visible in the last image, located north-east of the crater wall.

CHAPTER 5. CRATER ARELOGY QUALITY, RELATED TO SEASONAL ICE COVERAGE

Crater: 65N_210E

Location: 64.58°N, 209.64°E

This crater is located in the Vastitas Borealis region. The roughly 24 km crater is covered by two CTX images in total during the northern spring. During early spring the crater has ice coverage on the rim and on the dune field, with DDSs emerging them. The ice amount in the rest of the crater is hard to discern due to clouds covering it, but defrosting patterns and polygonal nets are visible. Later during spring the dunes are dark and almost no ice is visible in the crater, except on its rim and a thin ice layer on the north-eastern crater wall.

Crater: 65N_178E

Location: 65.12°N, 177.98°E

There are nine images covering the roughly 51 km large crater, whereof three images are taken by the HiRISE camera. The images are taken from the middle of the northern summer in Martian year 28 and reach to the middle of the summer, the year after, 159.6° to 124.4° in solar longitude. However, only one image is taken during the northern winter, 351.64° in solar longitude. Also, two of the images taken by the HiRISE camera have corresponding images taken by the CTX camera at that the same time, 159.6° and 131.8° in solar longitude.

During the summer in the Martian year 28, dust devils are visible in the middle of the crater, around the small peak. Also, some small dunes are located behind the peak, to the east. The crater is more or less uncovered by ice, but still, some small areas show traces of ice. When the winter then comes, a thin layer of ice seems to be covering the whole crater. However, larger stone formations on the crater floor are still visible through the ice. At this time, $L_s = 159.6^\circ$ in the Martian year 28, DDSs upon the dunes are observable. As spring turns to summer the following year, the ice sublimates to be visible only in hollowed areas on the crater floor.

Crater: 65N_128E

Location: 65.43°N, 128.33°E

There are six images taken by the CTX camera, over the roughly 29 km wide crater. The images are taken during the northern spring and reach to the middle of the northern summer, 37.43° to 146.09° in solar longitude. During the beginning of spring a thin layer of ice covers the crater. As the spring turns to summer, the ice layer has sublimated away and only a small amount of ice is left on the crater rim. In the latest image, in the middle of the summer, no ice is visible. In the middle of the crater a structure of polygonal nets and circular formations can be observed around its center. During the end of the spring dust devils have started to appear, which are still visible in the latest image, during the middle of the summer.

Crater: 66N_144E

Location: 66.38°N, 144.02°E

The CTX and HiRISE cameras have together taken four images of the almost 32 km wide, low-latitude crater. The images are taken from the beginning of the

northern spring and reach to the middle of the spring in, the same year, 13.07° to 61.1° in solar longitude.

The almost circular crater has a small peak in the middle with a couple of dunes upon it. In the beginning of the spring, a thin layer of ice covering larger parts of the crater is visible. The dunes in the middle have DDSs randomly spread upon them. In the middle of the spring, in the latest images, the DDSs are gone, as is the ice. Only small stripes of ice are visible, on the crater rim.

Crater: 66N_40E

Location: 66°N , 39.5°E

The roughly 37 km wide crater has five images taken by the CTX camera during the northern spring. The images are taken from the beginning of the spring and reaching to the middle of the northern spring, 26.75° to 59.43° in solar longitude. The peak in the middle has a structure of polygonal nets. South-west of the peak, a couple of ice covered dunes are located. In the beginning of the spring, ice is covering the crater and the dunes, except for some spots. As the spring goes, the ice sublimates. In the latest image, in the middle of the spring, the ice is still visible as a thin layer within the crater and as small stripes on the crater rim.

Crater: 66N_163E

Location: 66.35°N , 163.44°E

The approximately 24 km wide crater is located in the southern part of the northern hemisphere. Five images are taken by the CTX camera and one is taken by the HiRISE camera during the northern summer, reaching from 22.77° to 82.63° , in solar longitude. In the earliest image, ice is visible all over the crater. In the middle of the crater a small peak can be observed, and around this, a structure of polygonal nets. Also, the crater floor has some kind of heuchs around the middle region. Within these a structure of polygonal nets is visible as well. In the middle of the spring, 61° in solar longitude, there is a larger amount of ice covering the crater, compared to the image before. Almost no structure of the crater floor can be seen. The polygonal nets, visible earlier in the spring, can hardly be seen at this time. After this, the ice sublimates again and in the latest image almost no traces of ice are visible. Some stripes on the crater rim are visible in the east. Also, some dust devils have appeared in the middle region, north of the peak.

Crater: 67N_250E

Location: 67.12°N , 249.76°E

The roughly 25 km crater is covered by three CTX images from $L_s = 28.37^\circ$ to 63.22° . The crater is observed to have a polygonal patterned crater floor. Early in the spring the crater has a thin ice layer with defrosting patterns covering the whole crater. A thicker ice layer is located on the crater rim. An odd regolith feature is observed, and it looks like old frozen lava flow. During the middle of spring most of the ice has sublimed and only a thin ice layer is left on its rim.

CHAPTER 5. CRATER ARELOGY QUALITY, RELATED TO SEASONAL ICE COVERAGE

Crater: 67N_114E

Location: 67.09°N, 113.56°E

With six images in total, CTX and HiRISE have taken images of the roughly 22 km big crater from the beginning of the northern spring to the beginning of the northern summer, 28.55° to 110.10°, in solar longitude. In the western region of the crater, the crater floor has low circular formations. The crater has almost no ice covering during this time. Some traces of ice are visible on the eastern crater rim, but as the summer begins, the ice has sublimed away.

Crater: 67N_98E

Location: 67.13°N, 97.54°E

There are three images taken by the CTX camera of the almost 20 km wide crater. All of the images are taken in the beginning of the northern spring, reaching from 29.52° to 39.78°, in solar longitude. The crater floor is bubbly with surrounded darker lines and a structure of polygonal nets. A thin layer of ice is covering the whole crater at this time, although the structure of the crater floor is clearly visible. The latest image has, comparable to the earliest, less ice cover, which intends to defrosting.

Crater: 67N_93E

Location: 67.91°N, 92.84°E

Seven images in total have been taken of the roughly 29 km big crater. These are taken mostly during the northern spring but also during the summer, reaching from 21.42° to 123.56° in solar longitude. In the beginning of the spring, larger parts of the crater are covered by ice. DDSs are visible on the dunes, which are located between two stone formations/hills in the middle of the crater. Around the dunes, a structure of polygonal nets is visible on the crater floor. As the spring goes to summer, the ice sublimates, to eventually be almost gone at summer. Small stripes of ice are still left on the crater rim in the latest image.

Crater: 67N_252E

Location: 66.95°N, 252.05°E

The 9 km wide, simple crater has two images (one each by CTX and HiRISE) covering the whole crater during the northern spring, at $L_s = 43.7^\circ$ and 60.97° . The crater floor is covered by polygonal nets that are larger in size than those close to the bottom of the crater and smaller in size compared to those on the walls. The first image shows a partly thick layer of ice, located on the north crater wall, which thins out closer to the bottom of the crater. The polygonal cracks are observed to be filled with ice or frost. In the latest image more ice has sublimated and a thin layer is observed as a streak on the north crater rim.

Crater: 67N_223E

Location: 67.44°N, 222.89°E

On Scandia Colles, the approximately 14 km in diameter crater is located. This crater has three CTX images in total that cover the spring period, $L_s = 35.92^\circ - 68.19^\circ$. In all images the crater shows very small amounts of ice covering it. Most of the ice/frost is located as a thin layer on the rim or in the southern and eastern part of the crater. The ice undoubtedly sublimates with time, so that almost no ice is visible during the end of the spring. Features observed in the crater are polygonal nets that cover the crater floor. Dust devil tracks are observed in the latest image during spring over a dark region that probably indicates the location of dunes or dust.

Crater: 68N_190E

Location: 68.25°N, 189.6°E

The almost 12 km crater is located in the Vastitas Borealis region. The crater has five images in total covering it, thereof four CTX and one HiRISE images, taken between $L_s = 35.49^\circ$ and 135.8° . The earliest image has a thin cloud obscuring the bottom of the crater. However, there are polygonal nets visible, which are filled with ice in the hollowed out cracks. The polygonal nets on the crater floor are gone during the end of the northern spring and early summer. A large cliff is visible on the western crater wall. The ice thickness covering this cliff changes with time, from being thick to thin and then nothing. At the middle of the spring a lot of tracks of dust devils on the crater floor are visible, and no ice layer is visible in the high resolution image.

Crater: 68N_13E

Location: 68.31°N, 12.55°E

There are five images taken over the roughly 15 km large crater, whereof one is taken in high resolution. The images are taken during middle of the northern spring, reaching to the middle of the summer, 42.02° to 140.08° in solar longitude. There is a thin layer of ice, covering almost the whole crater in the earliest image. In later images the ice has sublimated away to only be observed on a small area, north-east, at the inner edge of the crater rim. With a structure of polygonal nets, the crater has an overall a smoother crater floor, compared to other craters.

Crater: 69N_26E

Location: 68.56°N, 26.46°E

Four images are taken from the beginning to the end of the northern spring, reaching between 28.19° to 82.8° in solar longitude. There are three images, taken by the CTX camera and one in high resolution by HiRISE, taken at the same time as one of the CTX images, 82.8° in solar longitude. The roughly circular crater is about 13 km wide and show a structure of polygonal pattern in the middle. The crater has almost no ice cover. However, a small amount of ice can be seen in small deeps on the crater floor and on the inner edge of the south-west crater rim.

CHAPTER 5. CRATER ARELOGY QUALITY, RELATED TO SEASONAL ICE COVERAGE

As the season goes toward summer, the ice amount eventually, in the latest image, become only a small stripe along the crater rim. Also, in the latest image dust devils have appeared in the south-western part of the crater.

Crater: 69N_41E

Location: 69°N, 41°E

There are two images taken of the roughly 20 km large crater. They are taken during the northern spring, 29.59° and 69.31° in solar longitude. The images are taken by the CTX camera and show, on the first image, a thin layer of ice/frost covering the crater and its small dunes, located in the north-eastern region of the crater. Behind the dunes to the west, a larger spot of ice is visible. Upon the dunes and on the ice spot, DDSs are visible. The crater floor is composed of a structure of polygonal nets. In the latest image, the DDSs on the dunes are gone, as is the ice spot behind them. The only ice left are small stripes located on the crater rim.

Crater: 70N_285E

Location: 69.50°N, 285.42°E

In south-west of Chasma Boreale, the approximately 20 km crater is located. Two CTX images and one HiRISE image cover the crater in total, during the northern spring between $L_s = 41.85^\circ$ and 70.07° . In one image, during the middle of spring, the crater is obscured by water-ice clouds, so the amount of ice covering the crater is hard to discern. However, by observing its southern rim, and just outside the crater, and comparing it with the other images, a thicker ice layer is present during this season. In the later two images the crater has almost no sign of ice, apart from the outer edge on the rim. This complex crater has a large area of dunes on the bottom and south-western crater wall. During the end of the spring the high resolution image shows that the large dunes start to become darker in color.

Crater: 70N_13E

Location: 70.05°N, 13.24°E

Three images are taken over the roughly 12 km big crater, whereof one is taken in high resolution. The images are taken during the middle of the northern spring, 44.9° to 62.16° in solar longitude. A thin layer of ice covers the whole crater in all the taken images. A bigger amount of ice can be seen in the south-west of the crater. As the time goes, the ice sublimates and in the latest taken image bigger areas of the crater floor is seen. Also, a structure of polygonal nets can be seen in the middle, together with a small crater impact in the south-west.

Crater: 70N_352E

Location: 70.03°N, 352.07°E

The crater is located in a region named Acidalia Planitia next to Vastitas Borealis. With 13 images in total, the almost 40 km crater has full image coverage of its total area. Five HiRISE and eight CTX images show how the seasons in the crater

change during one Martian year, reaching from solar longitude 24.91° to 349.8° . It is a complex crater with a flat floor having polygonal nets and dunes north of a concentric ring of peaks. Smaller craters are visible on the crater floor.

The earliest image, in (acquisition date) is from the end of the winter season, showing a totally ice covered crater, partly obscured by thick clouds. During early spring a thick ice layer covers the whole crater together with its gullies, located on the eastern side of the crater. Defrosting patterns start to form as ice starts to sublimate during the middle of the spring, and with it dark features start to form on the dunes. The ice layer on the crater wall and on top of the peaks in the bottom of the crater gets thinner at this time.

Until the beginning of summer the dunes are ice covered, which is clearly visible as the dunes become darker when they become exposed. Images from the end of spring show that most of the ice has sublimated from the crater wall, the rim and the bottom of the crater. There is only some ice left on the dunes. During the beginning of summer, dust devils have left tracks on and close to the dunes, which are not clearly visible during the middle of the summer.

Crater: 70N_267E

Location: 70.16°N , 266.55°E

South-west of Chasma Boreale, the almost 23 km crater is located. Eight images in total cover the crater, thereof four each from CTX and HiRISE, from $L_s = 27.4^\circ$ to 184.9° . This complex crater, having a peak in the middle, shows defrosting patterns early in the spring, $L_s = 27.4^\circ$. The thick ice layer becomes thinner and the ice movement can be observed. However, a large area in the southern part of the crater is still covered by a thick ice layer. High resolution images show thick ice layers on dunes with dark features around them. Also, odd features are visible, similar to polygonal nets, having white hills and darker valleys (which seems to be green/blue colored). Images during the middle of the spring show a partly ice covered crater with most ice, located on the crater wall and with some on the bottom of the crater. Almost no ice is observable in the crater during the summer. Only fragments of it exist on the western side of the crater, on the wall.

Crater: 71N_194E

Location: 70.55°N , 193.57°E

The roughly 36 km wide, complex crater is located in the area called Olympia Planum. Six images cover the whole crater during the northern spring season, whereof five of them are taken by CTX and one by HiRISE. The high resolution image is taken during early spring, but the small area visible shows only a thin ice layer. This is strange. Some five solar degrees later, the crater is observed to have a very thick ice layer covering almost the whole crater. However, after five solar degrees again, the crater shows a thin ice layer. Defrosting patterns are visible in all images, more in the middle of the spring and less in the beginning and end of the spring, together with features as polygonal nets.

CHAPTER 5. CRATER ARELOGY QUALITY, RELATED TO SEASONAL ICE COVERAGE

Crater: 72N_146E

Location: 72.07°N, 145.91°E

The crater has two images taken during the northern summer, by the CTX camera, 42.02° and 61.55° in solar longitude, and one image taken in the northern summer in high resolution, 134.3° in solar longitude. The roughly 22 km large crater has a ragged crater floor with areas with a polygonal structure. Around the middle region, the crater has a heuch-like appearance and stripes towards the center. During the spring, the crater is covered by a layer of ice. However, the defrosting takes place and the structure of the crater floor can be seen. In the summer, the ice has sublimated and larger areas within the crater are uncovered.

Crater: 72N_144E

Location: 72.45°N, 144.20°E

The CTX camera has taken five images of the almost 21 km wide crater. The images are taken from the beginning of the northern spring and reaching to the beginning of the northern summer, 28.98° to 103.15° in solar longitude. Up to 63.8° in solar longitude, DDSs can be seen on the top of the dunes, in the north-east of the crater. Bigger areas within the crater are covered by ice. A bigger amount of ice is observed in the eastern part of the crater, from north to south. After this, the ice sublimates and the dunes have no longer any DDSs. The dunes and the crater are almost uncovered by ice. In the later images, in the beginning of the summer, only stripes of ice are visible on the crater rim. Also, some dust devils have started too appear in the middle, around the dunes.

Crater: 72N_345E

Location: 71.53°N, 344.83°E

Located in an area called Vastitas Borealis, the crater is roughly 22 km wide. It is covered by two CTX and two HiRISE images during $L_s = 42.2^\circ$ to 129.6° . During the middle of the spring the crater has an overall thin ice layer except on the dunes and on the western crater wall, which have a thicker ice cover. Gullies are visible on the western side of the crater rim. The gullies, which could be dried out channels from water, of which only the lower parts are ice covered at this time of season.

During late spring the gullies have absorbed ice and now have a thicker ice layer covering them. A thin cloud is obscuring the crater bottom, but the white dunes and the DDSs appearing upon and around them are still visible. It is clearly noticeable that a large amount of ice has Sublimated from the crater rim and partly on the crater wall, but especially outside the crater. The high resolution image taken during the beginning of summer, shows that the western crater wall and half of the dunes are visible. At this season thin spots of ice are only visible in hollowed out areas and on the rough crater wall.

Crater: 73N_2E

Location: 73.35°N, 2.21°E

The roughly 17 km large crater is covered by three images. All of the images are taken during the northern spring, reaching between 15.70° and 66.21° in solar longitude, whereof two images are taken, almost at the same time, 15.7° in solar longitude. One image is taken by the CTX camera, the other one is taken in high resolution by HiRISE. The crater is more or less completely covered by ice. In the earliest images DDSs have started to appear on the southern edge of the dunes, in the middle of the crater. Also, defrosting patterns are clearly visible on the dunes, as a cracked covering structure. In the latest image, larger areas in the crater, as well as some of the dunes are uncovered by ice. The DDSs on the dunes, seen on the earlier images, are gone, and a structure of polygonal nets can be seen on the inner edge of the crater rim, together with small amounts of ice.

Crater: 73N_22E

Location: 73.12°N, 21.53°E

There are two images taken of the roughly 12 km large crater. One is taken by CTX and one in high resolution, by HiRISE. Both images are taken during the same time in the middle of the northern spring, 43.1° in solar longitude. The crater is more or less empty at this time. Small amounts of ice can be seen on and behind the crater rim. The crater floor is rugged with polygonal nets in the southern part of the crater.

Crater: 73N_27E

Location: 72.59°N, 27.11°E

There are two images taken of the roughly 17 wide crater. The images are taken by the CTX camera during the middle of the northern spring, 48.89° and 68.43° in solar longitude. On the earliest image a thin cover of ice can be seen. This cover is almost gone in the latest image. In the later image the ice is only seen in small depths on the polygonal structure of the crater floor. Around the small dune formation in the northern part of the crater, DDSs are seen in the earlier image. Due to bad image quality in the latest image, the DDSs are not confirmed to be present.

Crater: 73N_178E

Location: 73.4°N, 178.22°E

Four images are taken over the roughly 22 km wide crater, whereof one is taken in high resolution with HiRISE. The images are taken during the northern spring, between 39.7° and 61.96° in solar longitude. At $L_s = 39^\circ$, the crater is covered with one image taken by the CTX camera and one image in high resolution, by the HiRISE camera. In the images, a small peak in the middle, covered with polygonal nets and small amount of ice is visible. In the north-east, behind the peak, an area with dunes is located. At this time, defrosting patterns are visible like a cracked covering surface on the dunes. Above and behind the dunes, DDSs have

CHAPTER 5. CRATER ARELOGY QUALITY, RELATED TO SEASONAL ICE COVERAGE

appeared as well. The crater has a thin layer of ice covering it. In the direction of the north-western crater rim, the ice amount is less, compared to the rest of the crater.

Crater: 74N_187E

Location: 73.52°N, 186.81°E

In the area called Olympia Planum the roughly 26 km in diameter crater is located. Four CTX images in total cover the crater during middle and late northern spring, $L_s = 35.49^\circ - 70.03^\circ$. The crater has a peak in the middle, as complex carvers do, with dunes and polygonal nets covering it (strongly visible during the middle of the spring).

During the early spring the crater has a thin ice layer covering the whole crater, including the dunes, with DDSs upon and around. In the middle of spring, two images show how the crater has clear defrosting patterns, as wavy layering of ice caused by ice movement. At some areas on the crater rim and wall, the ice has Sublimated completely, and bare regolith emerges. At $L_s = 70.03^\circ$ the crater is almost empty of ice. The dunes are uncovered by ice and have become darker. On the southern and western rim of the crater, a thin ice layer and spots can be seen.

Crater: 74N_347E

Location: 74.38°N, 346.84°E

The roughly 22 km crater is located at Vastitas Borealis. There are three images in total covering the crater between $L_s = 27.29^\circ$ and 99.2° . The earliest image shows thick ice coverage over the whole crater, including the large dune formation in the middle of the crater. Dark features are visible at this time, north of the dunes. In the middle of spring defrosting patterns are clearly visible. The ice is thinner and ice layering has been created on the crater walls. However, the dunes are still ice covered, but DDSs have appeared around them.

Crater: 74N_13E

Location: 74.43°N, 13.24°E

There are three images covering the crater. One image is taken by the CTX camera during the northern winter in Martian year 28. The other two images are taken almost at the same time, during the northern spring in Martian year 29. One is taken by CTX, the other one by HiRISE. The diameter of the crater is about 12 km. The crater is more or less covered by ice in the earliest image. However, DDSs can be observed, upon and behind the dunes, which are located north-west of the crater. The later images show DDSs, together with defrosting patterns and less snow, compared to the first image. Small amounts of ice can be observed in small hollowed out areas within the crater. Also, a larger amount of ice is still left on the inner edge of the north-eastern crater rim. A hint of polygonal nets can be observed on the rugged crater floor.

Crater: 74N_319E

Location: 74.16°N, 319.49°E

This crater is roughly 17 km in diameter and located near the region Chasma Boreale. Its four CTX images taken during $L_s = 14.31^\circ$ and 72.1° show the effect of ice sublimation on the large field of dunes, covering almost the entire crater floor. In the early spring the whole crater wall has a thin ice layer. The dunes are totally ice covered, but the cover is thin enough to show the black feature spots on the dunes, below the ice. During the middle of spring the thin ice layer on the crater wall has become thicker, due to condensation of ice, and the dunes show an increased amount of DDSs.

During the late spring defrosting patterns are visible and a large amount of ice has sublimated and made the ice cover to disappear on the northern crater wall. The dunes have a thin ice layer, if any, at some areas. The DDSs have increased. In the last image at the late spring, almost no ice is visible on the dunes, which have become dark (as how sand becomes when wet). Ice is only visible on the top of the rim, which decreases in amount and thickness downwards to the bottom of the crater.

Crater: 75N_15E

Location: 74.52°N, 14.59°E

The crater is located in the Vastitas Borealis region, also referred to as the northern lowlands. The images are taken during the middle of the northern spring and reaching to the beginning of the northern summer, 47.68° to 94.13° in solar longitude. There are four images taken over the crater, whereof one in high resolution is taken at the same time as an image taken by CTX, 94.1° in solar longitude. The crater has a rough diameter of 12 km and is in the earliest image, covered by a thin layer of ice. On and behind the dunes, located in the middle of the crater, DDSs can be seen. As spring goes to summer, the ice sublimates away and a structure of polygonal nets can be seen on the crater floor, around the dunes. In the latest images the dunes are uncovered and only small amounts of ice is left. Some of the DDSs are still left, located behind the dunes.

Crater: 75N_340E

Location: 75.3°N, 340.49°E

Between the areas called Vastitas Borealis and Gemina Lingula, this crater is almost 16 km in diameter. Two images from CTX cover the crater in the beginning, $L_s = 21.57^\circ$, and in the end, $L_s = 81.3^\circ$, of the northern spring. In the first image, the crater is almost completely ice covered. The eastern crater wall and rim has a thicker ice layer compared with the opposite side. The very large dune formations located on the bottom of the crater and western wall, are ice covered with dark features emerging on and around them. At the end of spring the dunes are dark, having some ice cover on the outer edges of the high dune peaks. Over all, the crater shows almost no sign of ice, except on the highest point on the rim.

CHAPTER 5. CRATER ARELOGY QUALITY, RELATED TO SEASONAL ICE COVERAGE

Crater: 75N _ 158E

Location: 75.31°N, 158.28°E

The roughly 14 km crater is located in the Vastitas Borealis region. It is covered by five images between $L_s = 40.62^\circ$ and 138.34° . During early spring, the crater is covered by a thick ice cover, which is observed to be a mixture of carbon dioxide and water, the CTX camera at this time. However, defrosting patterns are visible, during the whole northern spring and summer. The crater has a structure of polygonal net as a floor. During the end of the spring and the middle of summer, ice has sublimated away from the northern crater wall, and left a partially thin ice layer.

Crater: 76N _ 159E

Location: 76.00°N, 159.00°E

There are three images covering the roughly 14 km wide crater. All of the images are taken by the CTX camera in the middle of the spring and in the middle of the summer, reaching from 40.62° to 138.34° in solar longitude. During the northern spring, a thin layer of ice is visible over the rugged crater floor. As the spring goes to summer, the ice sublimates, to be visible only in the south-western part of the crater, in the middle of the summer.

Crater: 76N _ 333E

Location: 76.18°N, 332.8°E

Just above the area Vastitas Borealis is the almost 12 km crater located. It has three images in total, all taken with CTX during spring at $L_s = 33.9^\circ$, 46.37° and 61.31° . In all images, the crater has ice on its rim, more during early spring and less during late spring. The large field of dunes at the bottom of the crater is not covered by ice in any images, but shows an increase of DDSs with time together with defrosting patterns. However, at $L_s = 46.37^\circ$ the crater adsorbs a thick layer compared with the previous image, and cause the DDSs to decrease in size and amount.

Crater: 77N _ 196E

Location: 77.2°N, 195.79°E

Located in the region called Olympia Planum, this approximately 22 km crater is covered by four CTX images between $L_s = 28.91^\circ$ and 125.86° . A thick ice layer is visible, covering the crater and the dunes at the bottom of the crater. The dunes have visible DDSs emerging upon and around them, which increase in amount and size with increasing solar longitude during spring. During the middle of spring, this expansion of DDSs has reached the crater wall, together with visible defrosting patterns. At the end of the spring defrosting patterns are emphasised and at the north-east crater wall almost no ice is left. During the middle of the summer, all ice has Sublimated from the northern part of the crater, including the dunes. Only a thin layer of ice starting from next to the dunes and going toward south is left, and has visible patterns of defrosting.

Crater: 77N_90E

Location: 77.54°N, 90.43°E

The roughly 34 km wide crater is covered by images taken by both CTX and HiRISE. Most of the images are taken during spring and summer, reaching from the middle of the northern summer in Martian year 28 and to the beginning of the northern summer in Martian year 29, 145.92° to 113.5° in solar longitude. In Martian year 29, two of the images are taken during the northern winter, 349.11° and 351.76° in solar longitude.

During the northern summer in Martian year 28 the crater is more or less completely covered by ice. Only a small part between the ice within the crater and the crater wall are visible. During the winter, the whole crater is then covered. Only a vague formation of the crater is visible.

In the spring of Martian year 29, the crater is completely full of ice. Defrosting patterns are seen in the south-western region of the crater. In the middle of the spring the crater rim is more visible in south-west. Behind the crater, a lot of dunes are located. At this time of the year, DDSs have appeared. Compared to the images taken during the winter, the ice amount has decreased a lot within the crater.

During the second part of the spring, defrosting patterns are clearly visible. Between 59° and 69° in solar longitude, the crater seems to have been covered by frost. Visible part of the south-west crater rim that was uncovered in $L_s = 59^\circ$, are covered again in $L_s = 69^\circ$. After this, the ice is again observed sublimating and the crater rim becomes visible. In the end of the spring and in the beginning of the summer the whole crater rim is visible, and some small regions of the crater floor can be vaguely indicated.

Crater: 77N_46E

Location: 77.00°N, 46.00°E

The small and almost 11 km wide crater is located within a region of dune fields, Siton Undae. The images are taken by the CTX camera during the winter in Martian year 28, and reaching into the start of the northern summer in Martian year 29, 350.34° to 116.68° in solar longitude. During the Martian winter the whole crater is covered by ice. Covered dunes are located in the north. Behind the dunes, to the south, DDSs can be observed. In the middle of the spring the DDSs have started to appear upon the dunes as well. Strong defrosting patterns are visible in the whole crater. In the latest image, in the beginning of the summer, the dunes are uncovered, and like a road, a line from the south-west crater rim towards the dunes, is free of ice as well.

CHAPTER 5. CRATER ARELOGY QUALITY, RELATED TO SEASONAL ICE COVERAGE

Crater: 78N_52E

Location: 78.01°N, 52.35°E

There are four images taken of the roughly 16 km wide crater. All of these are taken by the CTX camera during the northern spring and summer. One image is also taken during the northern winter in Martian year 28. The images cover the crater from 28.62° to 114.78° in solar longitude.

During the summer of Martian year 28, everything except for the dunes in the west of the crater is covered by ice. Some traces of dust devils are visible towards the west. In the image taken during the winter, the whole crater is covered by ice. Early in the spring, the following year, the crater is still covered, but all over the dunes, DDSs have appeared. When the summer then comes, the DDSs are still visible. Defrosting takes place and the crater floor has started to become visible in the northern part of the crater. Except for this region, the crater is still covered by ice in the latest image, in the beginning of the summer.

Crater: 78N_41E

Location: 78°N, 41°E

Five images taken by both CTX and HiRISE cover this mid-latitude crater. The images are taken during summer and winter, in Martian year 28 and during spring in Martian year 29, 146.51°, 352.36° and between 42.6° to 62.57° in solar longitude, respectively. The crater is roughly 14 km in diameter and has dunes located in the western region. During the summer, in Martian year 28, the crater is uncovered by ice until later into the winter, when it becomes totally covered. When the spring comes the following year, defrosting features are visible on the surface of the dunes, similar to a cracked surface. Upon this, black features are randomly spread on the dunes. Also, a structure of polygonal nets is visible on the crater floor around the dunes. In the latest image, in the middle of the spring, the DDSs are still visible together with a larger amount of ice within the crater. However, some of the ice is gone in the northern part of the crater.

Crater: 78N_346E

Location: 78.38°N, 346.93°E

The crater is located just under an area called Gemina Lingula. Three CTX images in total cover the crater, during the middle of the Martian spring and summer, reaching from $L_s = 35.28^\circ$ to 138.88° . The crater is 9 km in diameter and is observed to have a large amount of ice left in the western part of the crater during the middle of the summer. This could be residual water ice. The frost/ice outside the crater is observed to behave very strangely. On the outer western side of the crater, the area is bare and the eastern side is ice covered in the shape of a half circle embracing the crater. This behavior could be due to wind direction, blowing the ice in the same direction, or due to a warmer spot being present to the west of the crater, not letting frost deposit place there. During the middle of the spring, the crater is full with ice.

Crater: 79N_62E

Location: 79.00°N, 62.00°E

The crater is located in an area with dune fields, called Siton Undae. There are eleven images taken of the almost 18 km large crater. The images are taken from the middle of the northern summer in Martian year 28 to the same time the following year, reaching from 145.96° from one year to 145.65° in the other, in solar longitude. Three of the images are taken during the winter at the Martian turn of the year, 28/29. The crater is completely full of ice during the winter, the crater rim and the dune formations, located in the middle region of the crater, can hardly be distinguished. As early as three degrees in solar longitude, DDSs have started to appear on the dunes. In the middle of the spring a cracked surface can be observed on the dunes together with DDSs.

In the middle of the northern summer, defrosting takes place in the whole crater, and larger parts of the dunes are visible, but still some of the DDSs are also visible. Also, the north-eastern crater wall has become uncovered. In the latest images, during the middle of the northern summer, half of the northern region of the crater is uncovered by ice, like the dunes.

Crater: 79N_240E

Location: 78.7°N, 240.46°E

Six images in total cover this roughly 16 km crater during $L_s = 43.28^\circ - 350.48^\circ$. During the middle of spring, the crater has a thin ice layer covering its walls. At the bottom of the crater, a large dune formation is observed that is partly ice covered, with many dark features upon and around the crater. High resolution images show polygonal patterns covering the crater floor next to the dunes. Later during spring, it is observed that the ice has sublimated firstly from the northern crater wall and from the rim. However, it is observed that ice has accumulated on the western part of the dune formation. During the northern winter the crater is fully ice covered by a thick layer.

Crater: 81N_117E

Location: 81.36°N, 117.28°E

There are two images taken of this high latitude crater. They are taken from the CTX camera during spring and summer, in two different years, 116.11° in Martian year 28 and 62.74° in Martian year 29. The crater is almost 12 km wide and completely covered by ice. Defrosting patterns are visible in the northern part of the crater, during spring. Also, a couple of DDSs are visible on the ice in the middle of the crater, but also outside, behind the crater, to the west.

5.2 Named craters in alphabetic order

Crater: Boola

Location: 81.15°N, 254.84°E

Very close to the NPRC is the roughly 15 km Boola crater located. It is covered by two CTX images from the middle of the Martian spring and summer. During the middle of spring, Boola seems to have a large amount of ice at its bottom and a thick ice layer on the eastern crater wall. The rest of the crater has a thinner ice cover. During the middle of summer defrosting patterns are visible and a large amount of ice has Sublimated away. Spots of ice are visible on the rim, and a large area of thick ice is left at the bottom of the crater, which could possibly be visible residual ice.

Crater: Crotone

Location: 82.18°N, 298.59°E

The roughly 17 km crater is located in the Chasma Boreale region. It is covered by two CTX images during the Martian spring and two images during the summer. At $L_s = 51.41^\circ$ and 53.68° the crater has a thick ice layer covering the whole crater. Defrosting patterns are visible on the north-western crater wall, where ice movement can be observed from the shape of horizontal stripes or waves, which appear darker than the area surrounding it. During the middle of summer the crater rim has a thin ice layer covering it with spots of thicker layering. The darker stripes surrounding the inner crater are very strange. It could be the crater floor having this shape, or it could be an aged thick layer ice left annually, and partially being frost covered by a thin layer during summer.

Crater: Dokka

Location: 77.10°N, 214.46°E

The roughly 45 km Dokka crater, is located at the Olympia Undae region. It is covered by five CTX images between 12.48° and 353.16° in solar longitude. In the earliest image, the whole crater is covered by a thick ice layer. In the middle of the spring defrosting patterns are visible. Ice has Sublimated more on the southern rim of Dokka, and made the ice layer thinner, making some spots disappear. During the Martian winter season a large amount of ice has accumulated on the whole crater surface and rim, making the ice layer thicker.

Crater: Escorial

Location: 77.03°N, 305.17°E

In the Chasma Boreal is the roughly 17 km Escorial crater located. It is covered by three CTX images during the northern spring. At early spring the crater has a thick ice cover on its wall and rim, but the ice layer gets thinner to the bottom of the crater. The Escorial crater has a small peak at the bottom, and the rough crater floor has the patterns of long streaks, starting from the rim to the bottom of the crater. DDSs are visible on the western crater wall, even though no dunes

are visible. In images from late spring, these spots are gone, but leave a dark area behind, as dunes are observed to do in other craters. Also, time defrosting patterns are visible at this time, showing almost no sign of ice on the crater walls, except on the rim.

Crater: Heimdal

Location: 68.20°N, 235.72°E

The almost 10 km crater, Heimdal, is located in a region called Scandia Colles. It is covered by 14 (nine CTX and five HiRISE) images in total during spring and summer, between 37.29° and 154.30° in solar longitude. During the middle of spring, the crater has a thin ice layer on the north-eastern and southern crater wall, which increases in amount radially upward to the top of the rim. The crater floor is rough and has a bubbly pattern. High resolution images show odd DDSs appearing as spots on the crater floor. They are similar to shadows and unlike those DDSs commonly observed on dunes. With solar longitude, the ice sublimates and leaves almost a naked crater floor behind, with some spots of ice on the southern and north-east wall. Later during spring, polygonal nets are visible.

Crater: Inuvik

Location: 78.6°N, 331.4°E

Just below the Chasma Boreale, the almost 20 km Inuvik crater is located. Nine (seven CTX and two HiRISE) images in total cover the crater between 21.09° and 145.05° in solar longitude. During early spring Inuvik has a thick ice layer covering the whole crater, including its large field of dunes located on the western crater wall and floor. The dunes have at this time DDSs on and around them. Later, closer to the middle of the spring, DDSs have emerged on the crater walls as well, which is very uncommon. Defrosting patterns are seen close to the dune formations, as darker wave or stripe traces from ice movement. With time, still during the middle of the spring, defrosting patterns start to appear on the western crater wall, as the ice layer becomes thinner. Dune peaks are now darker compared to the surrounding area.

When the end of the spring is close, the dunes are showing large amounts of DDSs that slide downhill from the dune peaks, when the dunes are still thickly ice covered. As the temperature rises and ice Sublimates with increasing solar longitude, the ice layer gets thinner on the crater walls. However, the thick ice cover stays on the crater rim and bottom covering the dunes, which are still bleeding dark features.

As the northern summer gets closer, the thick ice cover vanishes from the large dune formations, and a thin ice layer of defrosting patterns surrounds it. A thin ice layer still covers the crater wall, but the thick ice cover is now gone from the rim, which now only has spots of ice covering it. In a high resolution image, a polygonal patterned crater floor is visible. During the middle of the summer the crater walls have no ice cover, and the dunes are dark without any DDSs. However, spots of ice are visible on the dunes and a larger amount of ice is visible to the north, west and especially to the south of the dunes. As the ice sublimates Inuvik's small crater peak in the centre becomes visible.

CHAPTER 5. CRATER ARELOGY QUALITY, RELATED TO SEASONAL ICE COVERAGE

Crater: Jojutla

Location: 81.33°N, 190.64°E

In the Olympia Undae region, close to the NRIC, Jojutla crater with its approximately 22 km in diameter is located. It is covered by nine (seven CTX and two HiRISE) images in total, during the middle of the spring and the middle of the summer. In the earliest images defrosting patterns are visible, and ice sublimation is clearly visible on the north-western rim. The large field of dunes on the bottom of the crater has a thick and fully covering ice layer, where DDSs have emerged and slid downhill from high dune peaks.

During the end of spring, defrosting patterns are visible and most of the ice has sublimated to a thin layer in almost the whole crater, except for the south-western crater wall, where a thick ice layer is visible. Strong winds have probably blown in the same direction, because hills, southern dune peaks and rough regolith all have a thick ice layer on their north-eastern side.

In the beginning of the summer Jojutla shows no ice layering in the northern part of the crater. Some spots of ice are left on the dunes but no DDSs are active. Only darker dunes are observable. The southern crater wall still has thick ice coverage, which gets thinner during the middle of the summer. Defrosting patterns are clearly visible during the whole summer on the southern crater wall.

Crater: Korolev

Location: 73.0°N, 164.5°E

With a diameter of almost 84 km in diameter, Korolev is the biggest crater on the northern hemisphere. There are 18 images taken by both the CTX camera and the high resolution, HiRISE camera. One of the images is taken during the northern winter, 350.6° in solar longitude. The other images are taken during the northern spring and in the northern summer, reaching from the middle of the summer in Martian year 28, to almost the same time in Martian year 29, 142.2° to 141.39° in solar longitude. Throughout the Martian year, Korolev is observed with a bigger amount of ice on the crater floor, probably residual ice. The earliest images show defrosting patterns all over the crater. In the west of the crater something seems to be flowing under a dune-like material. The inner edge of the northern crater rim is uncovered, in contrast to the southern crater rim, which is covered by a thin layer of ice.

During the beginning of the spring in Martian year 29, the crater is completely covered by ice and earlier defrosting patterns are covered by a new layer of ice. However, DDSs are seen on the top of what could be dunes, in the southern part of the crater, 20.36° in solar longitude. In the end of the spring, 83.07° in solar longitude, sharp black lines have appeared in the cliff between the ice and the rim, located in the east of the crater. As the summer starts, these lines get fainter and the defrosting patterns are even more apparent. Even in the latest images there can be seen, as in the first images, something comparable to flowing under something dune-like, located in the north-western part of the crater.

Crater: Kunowsky

Location: 56.50°N, 350.58°E

At Vastitas Borealis region, the roughly 67 km crater is located. Kunowsky is covered by eight images taken between 16.7° and 351.92° in solar longitude, i.e., at early spring, beginning and end of the summer and winter season. Dunes are observed next to the circular group of peaks in the middle of the complex crater. There is not much snow or ice visible in this crater. Only thin layers are visible on the peaks, on the rough crater floor between the dunes, and partly on the crater rim. The situation does not change for the ice amount during early summer, but there are tracks of dust devils visible over dune formations. Images from the winter season show a fully ice covered crater, with a thick ice layer on the rim and crater floor and a thin layer of ice in hollowed areas and on the rough crater floor.

Crater: Lomonosov

Location: 64.95°N, 350.80°E

Lomonosov is located in an area named Vastitas Borealis. With 13 images in total, the roughly 112 km crater has close to full image coverage of its total area. Four HiRISE and nine CTX images show how the seasons in Lomonosov change during one Martian year, reaching from $L_s = 22.04^\circ$ to 352.44° .

Lomonosov is a complex crater with a flat crater floor and dunes next to a concentric ring of peaks. Smaller craters are visible on the crater floor, where the largest one has a diameter of 3 km. Five out of seven images from the middle of the Martian spring show that hollowed areas have hills of ice surrounding them. These hills become smaller with time, ice layers become thinner and dark dunes become more visible as ice sublimates. In the last images during spring, only the peak and some small craters next to it have a thick ice cover left.

Not much ice exists in the crater during summer, but at $L_s = 160.43^\circ$ ice is observed in valleys between dunes, which are small in size. Lomonosov has one image during winter, 352.44° , when the crater is fully covered by a thick water ice layer and a thinner carbon dioxide ice layer above it.

In all images covering Lomonosov during spring, defrosting patterns are visible. However, at the same time a strange behavior of frost is seen on the dunes and on the central peak, compared to the area around it. Four images have DDSs visible on the dunes at the crater floor. Two of them are from the middle of spring, 37.6° and 44.98° in solar longitude, and the other two during late summer, 151.5° and 160.43° in solar longitude.

Crater: Lonar

Location: 72.59°N, 38.27°E

Six images are covering the roughly 7 km crater, located at mid-latitude of the northern hemisphere. Two of the images, one by CTX, the other in high resolution, are taken during the same time in the middle of the northern spring, 47.2° in solar longitude. The other four images are taken during the middle of the northern

CHAPTER 5. CRATER AREOLOGY QUALITY, RELATED TO SEASONAL ICE COVERAGE

summer, reaching from 116.42° to 157.1° in solar longitude. Also, two of these images are taken at the same time, 157.1° in solar longitude, one by CTX and one by HiRISE, in Martian year 28. In the images taken during the summer in Martian year 28, only a small amount of ice can be seen in the east and in the south of the crater. During the northern spring, the year after, more ice is seen around and on the small peak in the middle of the crater. Also, a structure of polygonal nets can be seen on the peak. When spring goes to summer the same year, in the two later images, only a small amount of ice can be seen in the south, similar to the images taken in the year before.

Crater: Louth

Location: 70.16°N , 103.26°E

The roughly 36 km wide crater, Louth, is located three degrees lower in latitude compared to crater Korolev. There are 27 images in total, taken by both the CTX and the HiRISE camera. The images are taken from the middle of the northern summer in Martian year 28 and reaching to the middle of the summer in Martian year 29, 133.7° to 149.2° , in solar longitude. Throughout the Martian year, the crater has a slightly elliptical mound of water ice, located almost in the middle part of the crater. Except for this water mound, a small amount of ice is visible on the south-east crater wall and rim. In the eastern end of the water ice mound, some dune formations are visible. During the summer in Martian year 28 the crater is almost uncovered by ice except for a smooth cap of water ice mound in the middle and some ice on the south-east crater wall and rim. Also, in the western region of the water mound, it looks like some sort of dune formation is getting through the ice. Outside the mound the crater floor is composed by a structure of polygonal nets.

During the spring in Martian year 29 everything in the crater is covered by a thin layer ice/frost. DDSs are located on and behind the dunes, on the water ice mound. Defrosting patterns can be seen on the western part of the water ice mound, and along the crater rim. In the middle of the spring, 50.31° in solar longitude, larger parts of the dunes are uncovered by both ice and DDSs. Still DDSs can be seen behind the dunes, in the middle region of the water ice mound. Defrosting takes place, and larger parts of the crater are now uncovered except for the water ice mound in the middle and some ice in the south-eastern part of the crater. Also, defrosting patterns are visible on the water ice mound, especially from the middle towards the dunes in the north-east. Lines of defrosting are visible in the western region of the water ice mound, as well. In the end of the spring the dunes are uncovered and no DDSs are visible. The water ice mound is now comparable to a smooth cap of residual water ice. Also, some ice is still left on the south-eastern crater rim, comparable to the year before.

Crater: Puyo

Location: 83.79°N , 138.69°E

There is one image taken by the CTX camera of this high-latitude crater. The crater is roughly 10 km large. The image is taken during the middle of the northern summer. At this time the crater is covered by a layer of ice all over. Dunes located in the southern part of the crater are still covered, and DDSs can be seen on the

crater floor together with some parts of the crater floor that are visible through the ice cover.

Crater: Sevel

Location: 79.12°N, 323.85°E

South of the region called Chasma Boreale is the roughly 6 km Sevel crater located. It is covered by two CTX images in total from $L_s = 53.2^\circ$ and 109.9° . During early spring, Sevel is covered by a thick ice layer with DDSs visible to have emerged all over the crater, especially north of the crater. A strange behaviour of the ice is observed around the outside of the crater. The crater has a border of thicker ice layers embracing the crater in an oval shape. The area inside this oval (which is more visible during summer), has a much thinner ice layer or none at all during summer. This is a very odd behaviour, which could be due to wind directions, or an occurrence of higher thermal heat in some regions. During the early summer Sevel has a large and thick ice cover left in the bottom of the crater, which probably is annual residual ice. Defrosting patterns are visible in both images.

Crater: Udzh

Location: 81.98°N, 77.2°E

The high-latitude crater is located on the edge of the NRPC. There are five images taken by the CTX camera, covering the roughly 45 km wide crater. One of the images is taken during the northern summer in Martian year 28, 112.84° in solar longitude. The other images are taken during the middle of the spring and in the beginning of the northern summer in Martian year 29, reaching from 41.92° to 90.86° in solar longitude. The crater is almost completely full of ice during this period. Only small parts of the rim are visible and confirm the crater's existence. As spring goes to summer, starting in solar longitude 46.68° some hints of defrosting patterns can be seen in the southern part of the crater. In the beginning of the summer, defrosting is more apparent in the whole crater, but still the crater is completely covered by ice.

Chapter 6

Results

6.1 Ice amount in all craters

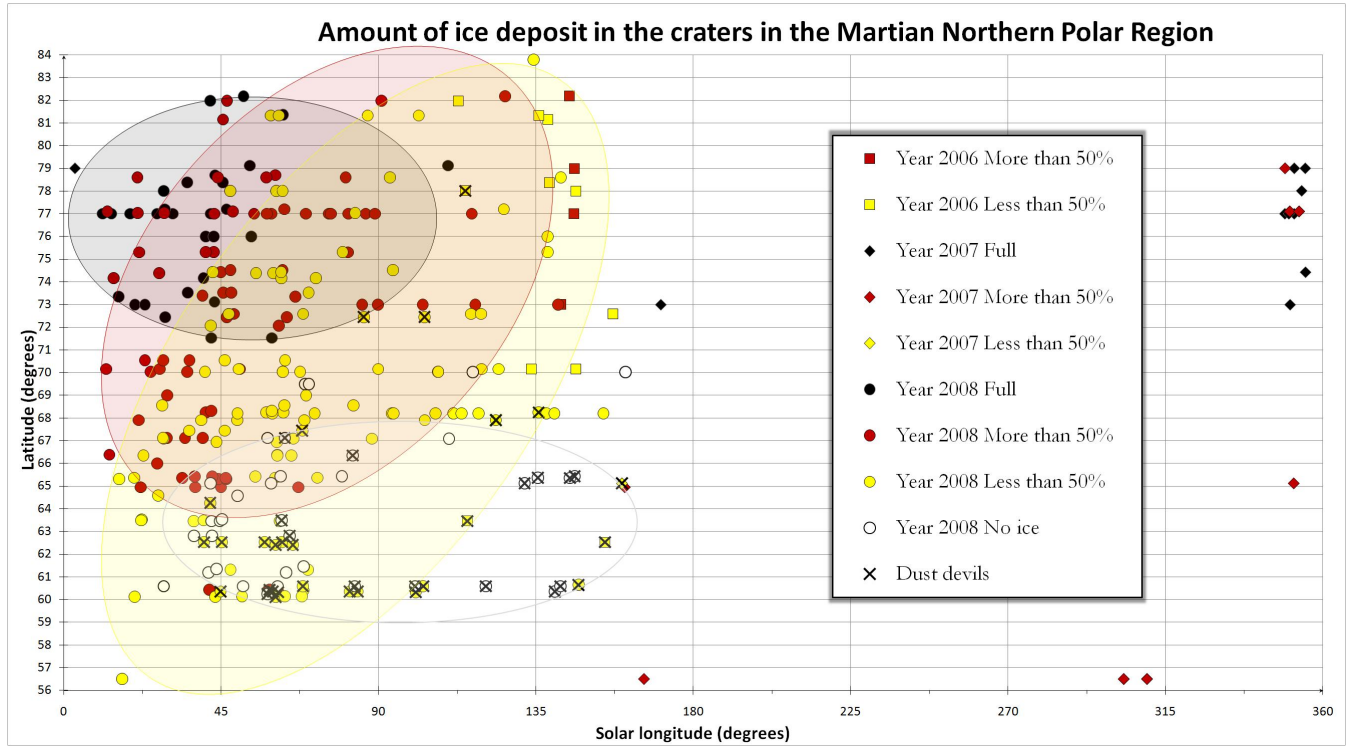


Figure 6.1: The ice coverage of the craters on the Martian northern polar region over different latitude and solar longitude. The white, yellow, red and black markings indicate when the crater has no ice, less than 50 percent ice, more than 50 percent ice or when it is full of ice. The green crosses represent observed trails from dust devils.

Figure 6.1 illustrates the amount of ice covering in all crater images taken during two Martian years, 28 to 29, which represent Earth years 2006 to 2008. Every dot represents an image of a crater, and its color represents the amount of ice, covering the crater at a specific time in solar longitude, L_s . The ice amounts in the craters are categorized in four different intervals, depending on how much ice covers the crater; full, more than 50 percent, less than 50 percent and empty. Here is no information about how deep this layer is. If the crater has a thin layer covering the whole surface of the crater, i.e., the structure of the crater floor is visible, the crater is set to have a full ice cover. If the crater is almost covered by ice, i.e., has small regions uncovered, the ice amount is set to more than 50 percent. If the crater has more regions uncovered, it is set to have less than 50 percent ice covering.

Overview analysis

According to Figure 6.1, there are images of craters with no signs of visible ice/frost within in them. This is within the range between 60° and 70° in latitude, during a seasonal period from the beginning of the northern spring reaching to the middle of the northern summer, 28° to 160° in solar longitude.

Images of craters with less than 50 percent ice are observed to be located in the range between 60° and 84° in latitude within a seasonal period between 15° and 158° in L_s . However, over the latitude range of 65° and 75° , during the same seasonal period, the craters containing less than 50 percent ice/frost are distributed denser.

The amount of ice follows a pattern illustrated with an ellipse with their respective color representing the ice amount. The crater images showing no signs of ice are basically observed on the lower part of the NPR during the end of the northern spring. The yellow ellipse represents crater images observed to have less than 50 percent ice coverage. Covering almost the whole NPR, it has a steep positive angle between 55° and 84° in latitude. The red and the black ellipse follow the outline of: with rising amount of ice in craters, the ellipse gets smaller in size and its central point increases in latitude and decreases in solar longitude.

The results acquired in Figure 6.1 are reasonable as colder temperature follows higher latitude. The closer the crater is located to NPRIC, located poleward of 80° in latitude, the more ice it contains. With increasing amount of ice, the ice will be preserved more or less the whole Martian year.

All of the observed craters are randomly located over the northern hemisphere. Figure 6.2 shows the relation between the location and the diameter of the craters.

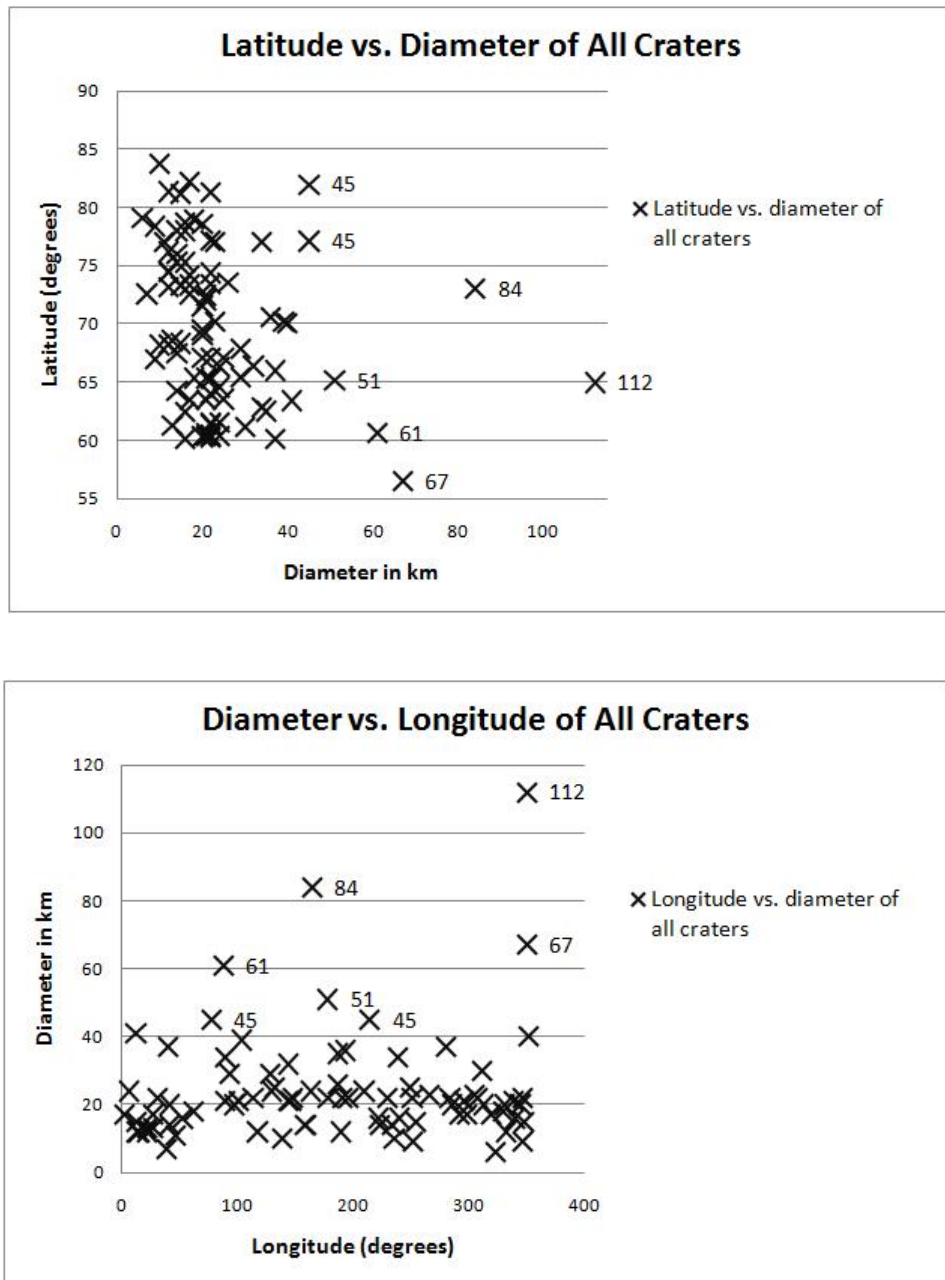


Figure 6.2: There seems to be no specific relation between the size in diameter of the craters and their location in latitude, nor in longitude.

As can be observed in Figure 6.2, most of the observed craters have an average diameter size between 10 and 60 km, randomly spread between latitudes 60° to 85° , all around the northern hemisphere, 0° to 360° in longitude. Of those craters, the average diameter is 20 km. Beyond those, there are three craters that have a larger diameter. The largest one is Lomonosov, with a diameter of 112 km, the second one is Korolev with a rough diameter of 82 km and the third one is Kunowsky with a diameter of almost 67 km.

Detailed analysis

From the overview analysis of ice amount, a detailed analysis of specific, unusual cases are analysed and compared with other craters, as described below.

- Two images of the same crater have more than 50 percent of ice coverage, during the middle of the northern winter at solar longitude 303° and 310° , at latitude $\sim 57^\circ$. This is an expected behavior for low latitude craters during this season of the Martian year.
- During a whole Martian year, images of the Lomonosov crater, $\sim 65^\circ$ in latitude, taken by both the CTX and HiRISE camera show more than 50 percent ice covering. However, during the northern summer, one of the images of the crater is observed to contain less than 50 percent of ice, at $L_s = 160^\circ$.
- Craters fully covered by ice can be observed between 71° and 83° in latitude, starting during the late winter season at $L_s = 351^\circ$ and lasting until middle of the spring, $L_s = 63^\circ$. One of these craters is Korolev, located 73° in latitude. Two observed images of Korolev are taken during the Martian year 28 and show a fully ice covered crater in the middle of the northern summer, $L_s = 141^\circ$. Still, in the middle of the northern spring, the year after, $L_s = 43^\circ$ Korolev is full of ice. The ice amount in the crater is observed to decrease with increasing solar longitude until $L_s = 141^\circ$, when the crater again is observed to be full of ice.
- Crater 79N_62E shows in late summer, in Martian year 28, an ice coverage that is more than 50 percent. The crater is full of ice between 349° and 3° in L_s , which is not surprising due to its high latitudinal location in the NPR.
- Sevel crater is another one observed with a large amount of ice. The crater is located at 79° in latitude and is observed to be full of ice in the middle of the spring and beginning of the northern summer at 53° and 110° . Due to its high latitudinal location this is unusual.
- At lower latitudes, craters are observed to contain less ice than those at higher latitudes. It is therefore more common to find craters at higher latitudes having residual ice annually, than those at lower latitudes. This pattern is clearly observed in Figure 6.1.
- Two craters, located on the eastern and the western side of the NPR at the same latitude and during the same Martian season, show a contrast in the observed amount of ice. One crater contains no ice and the other crater contains more than 50 percent.

As the northern summer reaches between 90° to 180° in solar longitude, a range from the middle of the northern spring reaching to the end of the northern summer has been taken to map craters with summer ice. To investigate if the amount of ice depends on the crater size in diameter, all craters observed to have ice deposits are plotted from their location in latitude as a function of the crater diameter in km. As observed in Figure 6.3, craters with no ice amount are low-latitude craters with a diameter size between 10 and 50 km. However, there exist craters at higher latitudes with no ice amount. These have a smaller diameter compared to craters with no ice amount at lower latitudes. Of all observed craters within this work it tends to be a decreasing diameter size of the craters with increasing latitude.

6.1. ICE AMOUNT IN ALL CRATERS

Craters with less than 50 percent ice amount seem to be randomly spread with an average diameter between 8 and 35 km, in latitude between 63° and 84° , while craters with more than 50 percent ice amount are located at higher latitudes with almost the same range in diameter. The information in Figure 6.3 indicates that a crater with bigger diameter at lower latitudes is able to retain ice during the northern summer.

Table 6.1 shows all observed craters with summer ice during the period 75° to 180° in solar longitude. All the images taken during this period are listed in Column 4, while the total number of images taken of the crater is listed in Column 5. Of all images that are taken during the period, $L_s = 75^\circ$ to 180° , the images that shows most ice amount are listed as a value, less 50 percent, more than 50 percent and full, in Column 3.

Overall there are 26 craters observed to contain summer ice during the period 75° to 180° in solar longitude. A few of these craters have full or more than 50 percent ice coverage, while, most of them have less than 50 percent ice coverage. At lower latitudes, less than 50 percent ice amount within the craters, are more common compared to craters located at higher latitudes. It is more likely to observe craters with more than 50 percent ice amount above 75 degrees in latitude, during this period.

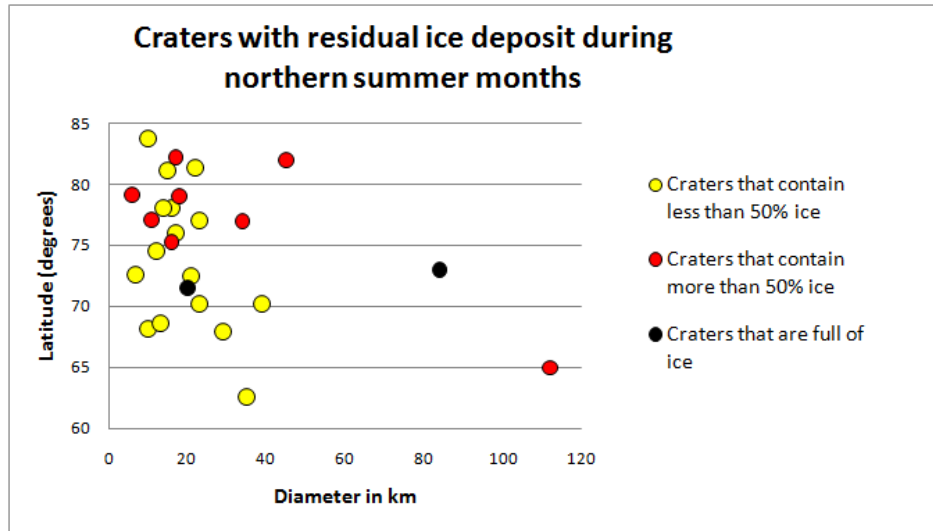


Figure 6.3: Low-latitude craters intend to have a larger diameter size to be able to retain more than 50 percent ice deposits during the northern summer.

Table 6.1: Ice deposits within craters during the summer months.

Crater	Latitude	Amount of ice	Number of images	Number of total images
62N_186E	62°	< 50%	1	5
Lomonosov	64°	> 50%	1	4
67N_93E	67°	< 50%	2	6
Heimdal	68°	< 50%	10	13
68N_26E	68°	< 50%	1	3
Louth	70°	< 50%	3	5
70N_266E	70°	< 50%	2	5
72N_215E	72°	< 50%	2	5
72N_38E	72°	< 50%	2	3
Korolev	73°	full	8	11
74N_14E	74°	< 50%	1	3
75N_340E	75°	> 50%	1	2
76N_159E	76°	< 50%	1	3
77N_89E	77°	> 50%	5	17
Escorial	77°	< 50%	1	3
77N_46E	77°	> 50%	2	6
78N_53E	78°	< 50%	1	4
78N_41E	78°	< 50%	1	3
79N_62E	79°	> 50%	1	5
Sevel	79°	full	1	2
Boola	81°	< 50%	1	2
Jojutla	81°	< 50%	3	5
Udzha	82°	> 50%	1	4
Crotone	82°	> 50%	2	4
Puyo	87°	< 50%	1	1

6.2 Dunes

In Figure 6.4 all the observed craters are plotted with latitude vs. diameter size. All craters that contain dunes are marked with a cross.

When comparing craters containing dunes with the craters diameter, a relation between them can be observed as a pattern. In the range between 56° and 84° in latitude, craters are observed to contain dunes. Of all observed craters within this work, none of the craters with less than 11 km in diameter contains any dunes.

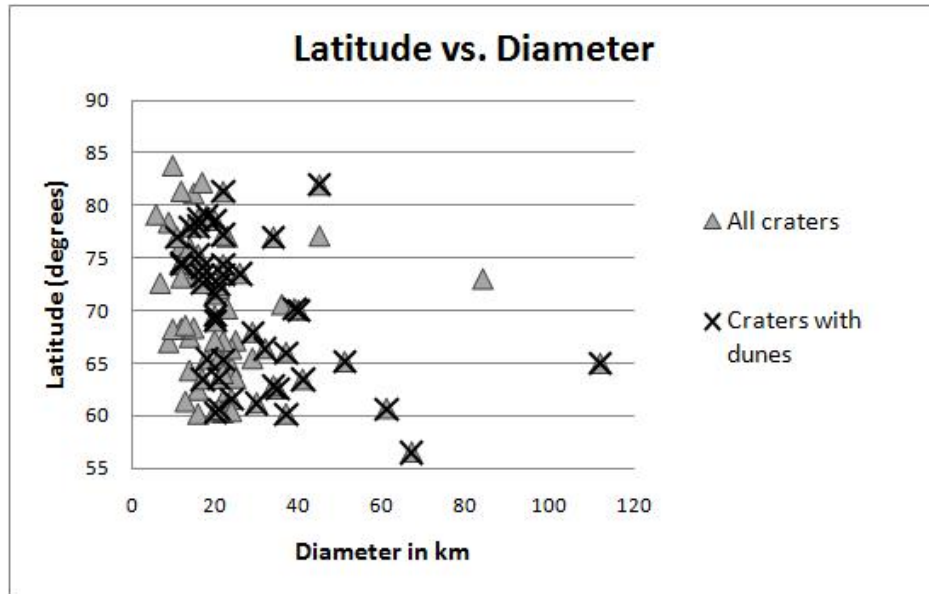


Figure 6.4: All observed craters together with those that contain dunes, marked with a cross, are plotted with latitude as a function of the crater diameter.

In Figure 6.5 craters containing dunes are colored in orange. The craters are observed to be almost randomly spread. But an indication of some sort of weak grouping can be seen.

Craters containing dunes seem to be located sparse and fewer between 135° and 270° in longitude. Also, between 0° to 90° , and 270° to 360° , in longitude, craters containing dunes seem to be located much denser.

6.3 Dust Devils

In Figure 6.5 all observed craters are plotted with their location in latitude and longitude. Craters that contain dunes and dust devils are colored in orange and black, respectively. Upon these markings, craters containing both dunes and dust devils are marked with a red cross, while craters containing no dunes but showing tracks of dust devils are marked with a blue cross.

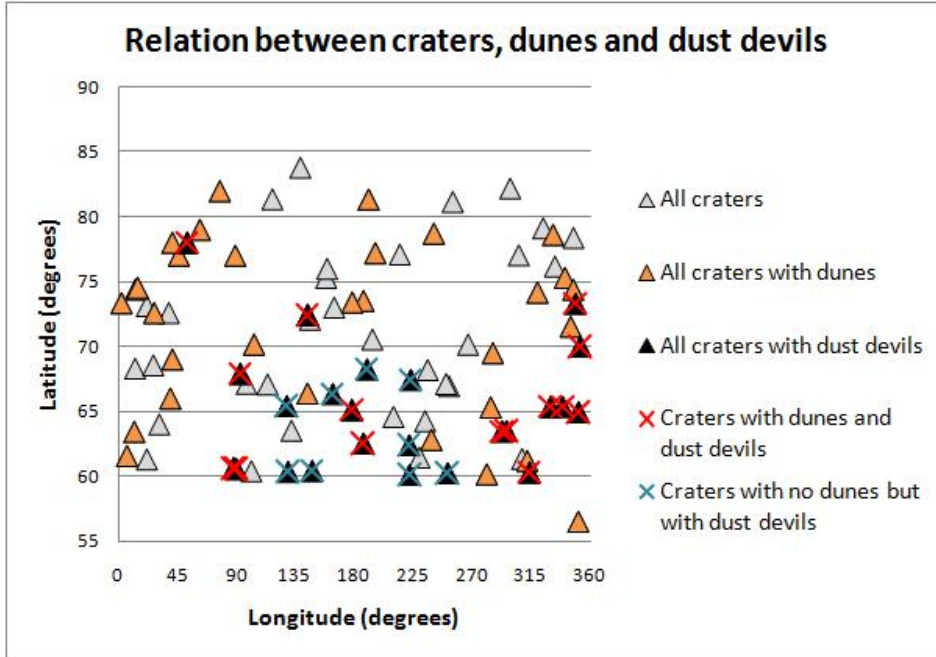


Figure 6.5: All observed craters and their dune and/or dust devil content at their locations in latitude and longitude.

Analyzing Figure 6.5, the dust devils seem to appear between 37° and 160° in solar longitude, during the northern spring until the end of the summer, over latitudes between 60° and 78° . No dust devils above 68° in latitude are observed in craters without dunes. Below 68° dust devils appears in craters both with dunes and without, randomly spread.

Craters without dunes but with tracks of dust devils can be seen only between 60° and 68° in latitude and between 128° and 251° in longitude. However, craters with dunes and visible tracks of dust devils are observed between latitudes 60° to 78° over a span of 52° to 352° in longitude.

Also, looking at the craters with dust devils and without dune formations, they seem to appear in the middle of spring and disappear at the end of the northern summer. Since dust devils are a result of temperature differences, this might indicate that dust devils depend of temperature. Early in the spring and the late summer, or in the beginning of the autumn, it might be too cold for dust devils to be created.

Many of the craters that contain dunes also show tracks of dust devils, but some of the craters that show tracks of dust devils, contain no dunes. Those specific craters have been plotted with latitude and solar longitude, from early spring to early autumn. As can be seen in Figure 6.6 most of the dust devils appear during the middle of the northern spring. A few can be observed during the middle of the northern summer at higher latitudes.

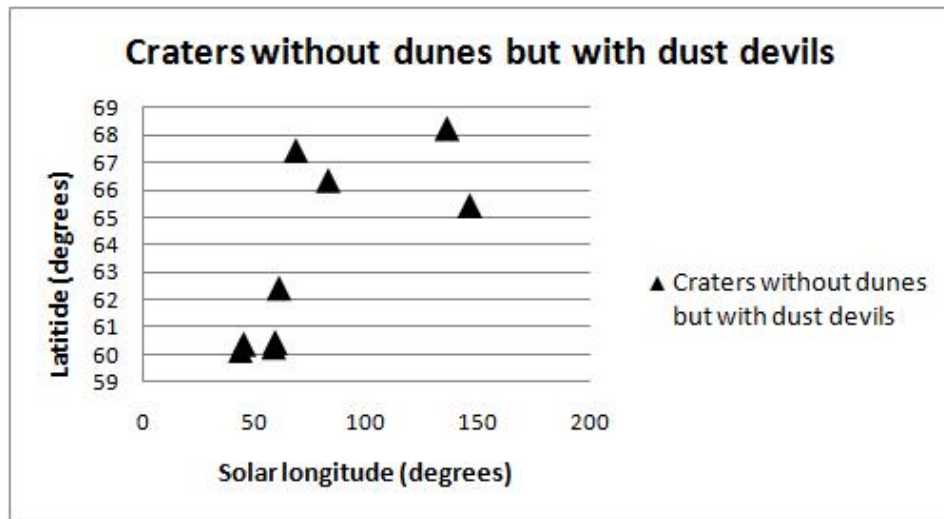


Figure 6.6: Craters that do not contain dunes have traces of dust devils. Most of them appear in the middle of the northern spring.

6.4 Defrosting features

Figure 6.7 illustrates when in solar longitude, and where in latitude, defrosting patterns are observed in all craters during two Martian years, 28 and 29. Every cross represents an image having visible patterns of defrosting.

Defrosting patterns appear in almost every crater, between 56° and 82° in latitude and between 10° and 160° in solar longitude. The relation of defrosting patterns with latitude and solar longitude seem to follow the shape of a thick arc, with its end starting from the origo, having its arc peak value at latitude of almost 30° and 78° , and ending roughly in $L_s = 77^\circ$ and $L_s = 145^\circ$. A dense and thick region of crosses dominates the central region of the arc, as can be seen in Figure 6.7.

Many craters at high latitude, $\sim 75^\circ$ poleward, are observed to have defrosting patterns early in spring at roughly $0^\circ - 40^\circ$ in solar longitude. These patterns were expected later in the spring, because of the craters location close or on the northern seasonal polar cap.

Two of the largest craters on the NPR, Korolev and Lomonosov have defrosting patterns late in winter, located at an altitude of 73° and 65° , respectively. Which is unusual, since defrosting patterns usually are observed during late winter and during spring.

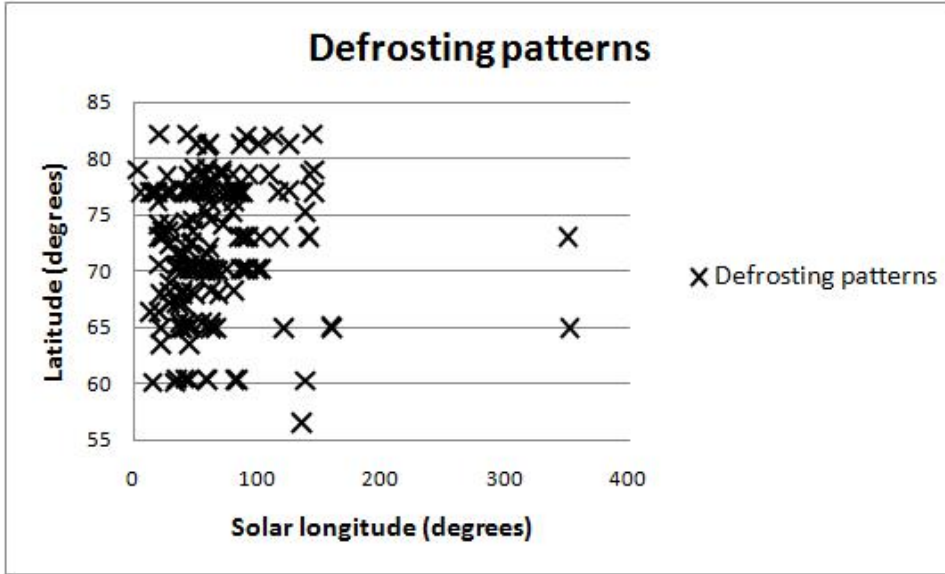


Figure 6.7: Every green cross represents the defrosting patterns in all crater images investigated in this work, taken throughout two Martian years, 28 and 29.

6.5 Dark dune spots

All craters in this work, with observable DDSs emerging on and next to the dunes, are illustrated in Figure 6.8, as a function of latitude and solar longitude. The black filled circles represent observable DDSs on the dunes in the crater, and the red crosses represent DDSs next to the dunes.

DDSs seem to emerge on and next to dunes within 0° - 150° in solar longitude, i.e., during early northern spring until late summer, and located between 60° and 82° in latitude. However, these patterns on and next to dunes are more common during the middle and the late spring season, $L_s = 0^\circ$ - 70° and are more densely located in a latitude gap between 60° and 82° .

In the craters 79N_62E, 77N_46E and 65N_182W, DDSs can be seen during the middle of the northern winter, at roughly the solar longitude 350° .

Overall, when DDSs are observed to appear upon the dunes during spring and summer, they are most likely observed next to the dunes as well.

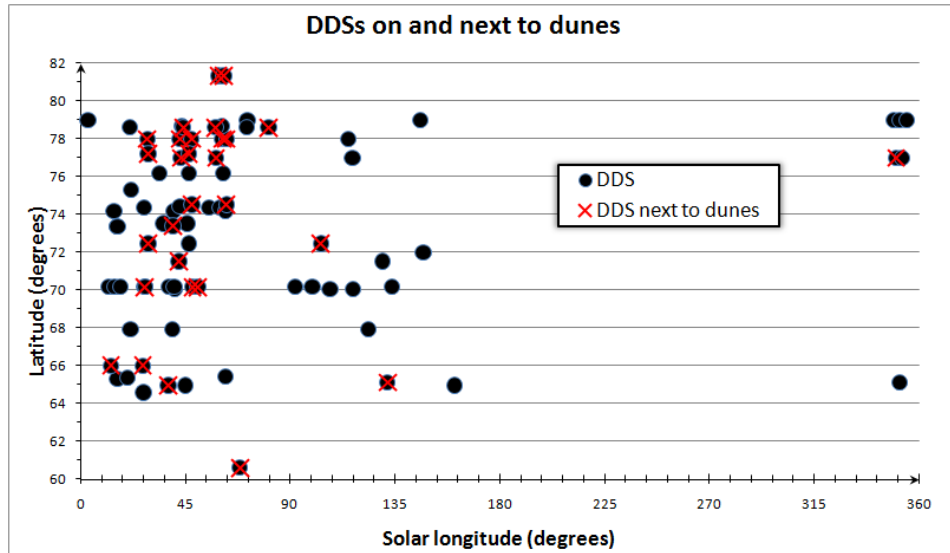


Figure 6.8: DDSs on and next to dunes, in latitude and solar longitude.

Chapter 7

Conclusions and discussion

For future Mars mission an understanding for the Martian environment is essential. In mapping and observing the craters on Mars NPR an understanding of the Martian history can be reached. In return, knowledge of why the Mars environment looks like it does today will be understood and a glimpse of the Martian future might be seen. By observing for example the dust devils, scientific questions will be answered about the Martian climate, i.e., the cycles of erosion and sedimentation and the surface-atmosphere interaction. A better understanding for the Martian climate will benefit future Martian robotic missions, but also possible human missions. Also, understanding the water and carbon dioxide cycle will give knowledge of what might have happened with the Martian atmosphere.

7.1 Ice amount in all craters

At lower latitudes, less ice is observable in the craters compared to higher latitudes. It is more common to find craters at higher latitudes being full of ice during all the Martian year.

Overall the ice amount in the observed craters follows a pattern, comparable to the one on Earth. But in contrast to the Earth, ices on Mars are sublimated instead of melting. As the northern spring goes to summer, both water and carbon dioxide ice is sublimated into the Martian atmosphere. As expected, almost all craters that are full of ice are high-latitude craters, located above 71° in latitude. During the northern spring these craters are full of ice, but as time goes, the ice sublimates. This is also true for craters that have more than 50 percent ice or less than 50 percent ice. But these craters are more sprawled, and depending on the size of the crater the ice amount within will be retained.

For craters to be able to retain ice they need to be located higher in latitude or have a larger diameter size. Small, low-latitude craters are more likely empty during all Martian year. If they contain ice, this will only be during a short period in the winter, and when the temperature will rise during the spring, the ice will be sublimated. Those low-latitude craters with summer ice are more or less bigger in diameter compared to the average size of the observed craters, i.e., Korolev and Lomonosov, where Lomonosov is the biggest, located at a lower latitude.

Impacts are often associated with a planets formation and evolution. But by analyzing the impacts, information of the subsurface can be known. For example, the fluidized ejecta, which can be observed around some craters on Mars, suggest the presence of volatiles, such as water or carbon dioxide in the subsurface.

By monitoring and analyzing the images of craters in the Martian NPR, especially ice covered craters like Korolev, a deeper understanding can be reached, of how water behaves on the Martian NPC and what kind of influence it has on the CO₂ cycle between the northern and southern hemisphere. To understand what might cause, for example, the change of the surface albedo in some craters, more images have to be taken in high resolution with HiRISE over different seasons, to monitor the change over time and what relation the change might have due to temperature. Also, by understanding all kinds of features that are observed within some of the craters, the science in astrobiology will develop and knowledge of the existence of life might be better understood. In mapping the craters on the NPR, more knowledge of the Martian history will be achieved which, in return, will be important for predicting the Martian future.

7.2 Dunes

Craters that contain dunes seem to be located sparse, and fewer are located between 135° and 270° in longitude. In contrast, between 0° to 90° and 270° to 360° in longitude, craters containing dunes seem to be located denser. Also, almost all observed craters located between 56° and 84° in latitude, contain dunes.

There are extensive dune deposits surrounding the NPR. Between 75° and 80° in latitude, the polar region is surrounded by crescentic dune material. While linear dune material, finely rippled dune formations, are adjacent near the cleft of Casma Boreale and the PLD in Olympia Planitia.

Of all observed craters in this work there are not many that are located in the region between 75° and 80° in latitude. There are roughly 16 craters located in this region, whereof the main bodies contain dunes. It has not been analyzed within this work what kind of dunes it is, but they are most likely crescentic or linear dune formations according to the work of Tanaka and Scott (1987).

If the craters contain dunes or not, most likely depends on where the craters are located on the Martian surface, as the terrain is different. Some regions of the Martian surface have different composition, depending on latitude. Due to the residual ice and the seasonal ice cap, the terrain is different compared to lower latitudes, with less or no ice deposits, which might influence if dunes will be created or not.

Dunes are known to be stable on Mars over time, but sometimes they move like dunes usually do on Earth. If dune formations are due to dust storms, it could be more dust storms in these specific regions, where craters with dunes are denser located.

Overall, craters containing dunes seem to be randomly sparse located over latitude, on the Martian NPR. Analyzing Figure 6.4, there seems to be no dunes within craters with a diameter of less than 11 km. Depending on how deep these craters

are, they may not have an enough high crater wall and rim to be able to hold the sand grains from being blown away by the wind. Compared to deeper craters, a higher crater wall and rim will enclose the dust grains from being blown away. Also, the size of the crater plays a role. Larger craters, with more area, will most likely be deeper, and have a higher crater wall and rim to enclose the sand. According to Figure 6.4, only one of the bigger craters, Korolev, lacks dunes. This crater could have dunes, but since it is more or less covered by ice the Martian year around, the lack of dunes, cannot be confirmed. However, as craters with larger diameters verify energy rich impacts, they also have a peak in the middle of the crater. Most likely a large crater is formed and that could be why smaller craters can not trap dust into the crater. This could be one reason why we do not observe any dunes within these craters. The formation of the crater impact might have an influence as well. Depending on the with what velocity the impact strikes the surface with, the crater floor will be composed differently and most likely affect how and if dunes are formed. Last but not least, one more factor affecting dune formations is the wind and its direction on Mars, which creates and shapes the dunes. Craters that seldom experience winds probably do not contain any, or few dunes.

7.3 Dust Devils

Throughout the work, dust devils have been seen randomly within the craters. They are observed mostly during the spring and the summer. The reason could be because the surface temperature is higher at this time of the year. The difference between the temperature on the surface and in the atmosphere will then become larger, and as a result of hot air rapidly rising will then cause a spinning effect of conservation of angular momentum. As the regolith and the dunes in the crater are no longer ice covered during spring and summer, the traces of the dust devils are more easily located, due to the wind that moves the dust particles and loose gravels more easily.

If the dust devils appear in craters with dunes, they will be more apparent, as loose grains of the dunes will be easily embedded in the vortices. Why craters containing dunes at higher latitude do not have any dust devils could be because at higher latitude, craters are more covered by residual ice and have a lower temperature, compared to those at lower latitudes. Also, if there would be a temperate rising on the surface, the dust devils will more likely not be seen because of the ice. Since the craters at higher latitude are covered by ice most part of the year, there is no sand or gravel for the dust devils to leave as traces.

Figure 6.5 shows how the dust devils are observed in craters without dunes. They seem to appear in the middle of spring and disappear in the end of the northern summer, 43° to 146° in solar longitude. This shows that our theory about the temperature dependence might be right. Early spring and late summer /autumn might be too cold for the dust devils to appear. But also, if the dust devil do not depend on the temperature they will not be seen on the images. Maybe in high resolution with HiRISE, if that is the case, there would be some kind of traces. Also, craters with dunes would be a source for dust devils to leave traces on nearby craters with no dunes. No such craters have been observed in this work. To find out more about the dust devils, how they appear, how they are affected, how they affect the surrounding, and what kind of traces they leave on the Martian surface,

more craters most be explored.

Some questions are not answered, for example, why do craters without dunes contain dust devils only at certain latitude and longitude, 60° to 68° , and 128° to 251° ? And what kind of influence do the dunes have for the dust devils appearance? In observing the dust devils, more knowledge can be achieved about the Martian surface, how the temperatures varies, and also how the Martian winds blow.

Our work has only scratched a little on the surface of what all the craters on Mars northern polar region contain, one of the studied features is the almost newly discovered dust devils, leaving black traces on the Martian surface.

7.4 Defrosting features

Defrosting patterns are observed to appear during $L_s = 0^\circ - 160^\circ$, as expected compared to similar patterns on Earth. Even though the resulting spread of crosses over season was expected, the latitudinal spread as a function of solar longitude was not. Many of the craters at higher latitudes show an early signature of defrosting during early spring. These patterns were expected later in the spring, because of the crater location close to, or at, the NSPC.

The necessary thermal radiation received from the Sun to sublimate carbon dioxide ice and later water ice, is expected to appear during the late spring or the beginning of the summer, compared with regions on lower latitude.

Anomalous seasonal behavior of ice in craters could also be explained by the type of ice covering it. Latitudinal variations in insulation which drives the atmospheric circulation of water, carbon dioxide and airborne dust (Jakosky and Haberle, 1992), affect the constitute of the ice, resulting in a mixture of water and carbon dioxide ice. This could be due to airborne dust that has settled on the ice after seasonal dust storms. These factors, in turn, determine the stability characteristics of the ice (Hale et al., 2005).

When ice becomes old (as the grains grow in size) (Murchie et al., 2007) or covered to dust, it will become darker and will then absorb more sunlight, thereby warming relatively quickly and defrost more rapidly (Calvin, 2008). The likely factors controlling ice accumulation, sublimation and defrosting are the surface properties, the length of day and night, distance to the sun, the solar angle, the latitude, the altitude, the clouds, the seasonal dust storms and the crater depth. These factors are described in more detail below.

The crater diameter is possibly a factor that can control the crater floor temperature. The temperature decreases with increased shadowing due to the diameter-to-depth ratio (Ingersoll et al., 1992). Shadowed areas are also a result of the solar angle, the crater location and the formation of the rim, if high or low.

Seasonal dust storms or local dust devils have airborne dust grains that absorb sunlight. These will heat the atmosphere locally, and the ice on which they have settled.

The effect of clouds on surface temperature is the net effect of three things; sunlight reflecting from their top side, the greenhouse effect of absorbing and radiating back the thermal radiation from the Martian surface, and the reflection of the thermal radiation from the surface back to the surface.

A large difference between day and night of the planet will cause the air to flow from the hot day side to the cool night side. These triggered winds, heated by the solar radiation, are called thermal tidal winds. Not only will ice rapidly sublimate and accumulate by this effect, but also the heated winds will be a probable source of dust storm and dust devil formations. The length the day and night will also influence the surface temperature. When Mars is near perihelion, during northern winter, the days are much shorter at the NPR, and as a result colder. This is, however reversed, during aphelion during the northern hemisphere winter.

With higher altitude and degree of latitude the temperature decreases rapidly to condensation temperatures of water, and especially to carbon dioxide condensation.

7.5 Dark Dune Spots

Most of the DDSs seem to appear in the spring and the summer. They are most likely related to defrosting as they appear during the same season. The first signs of emerging DDSs are observed during early spring.

In some craters, DDSs are observed to first of all appear next to dunes. Then as solar longitude proceeds, the number of spots increases and they start to appear upon the dunes as well. However, other craters show a different behaviour. DDSs are firstly observed on the dunes, and then they either vanish or grow in diameter with proceeding solar longitude. They then emerge on top of the dune peaks and slide down hills as the spots increase in diameter. During the end of the Martian spring until the end of the summer, DDSs start to disappear as they have finished developing. What was hidden under the ice emerges to the surface and reacts with the Martian atmosphere. At this point, when no new dark features can be produced due to ice sublimation, the dunes become dark in color, like wet sand on Earth.

DDSs observed next to dunes appear intensely during the middle and the end of the spring, over the span of $L_s = 20^\circ - 70^\circ$. Only two craters have DDSs appearing during summer. They are 72N_215W and 65N_182W, located at latitude 72° and 65° .

It is still not clear, why so few craters have DDSs appearing during summer, and why DDSs next to dunes disappear before those on the dunes. Maybe they can be explained by the surface and the low atmospheric temperatures, on the NPR.

Why and how these formations occur is still not clear. One hypothesis suggested by Appel et al. (2010) state that these dark features are all based on a solid state greenhouse effect. Their different appearances are explained as due to different terrains in which they occur. Depending on the composition of the dune, they consist of dark soil and sometimes finer grained soil that is bright when dry, but dark when mixed with water. During the beginning of the northern Martian spring

CHAPTER 7. CONCLUSIONS AND DISCUSSION

the dunes commonly have a layer of water ice with an additional layer of carbon dioxide ice. Possibly the surface is covered by a thin layer of bright, fine grained sand, which has been blown on top (Appel et al., 2010).

With spring, the temperature rises and the dune receives direct sunlight. The carbon dioxide absorbs nearly none of the solar energy through direct absorption, according to Hansen (2005). However, water ice absorbs parts of the IR spectrum, and consequently warms it (Grundy and Schmitt, 1998). The solar radiation will reach the darker soil, underneath the ice as well, which absorbs most of the solar energy and heats up faster than the surroundings. When the warmer soil heats the water ice just above it, a liquid interfacial layer will form between the water ice and the soil and mix them together (Appel et al., 2010).

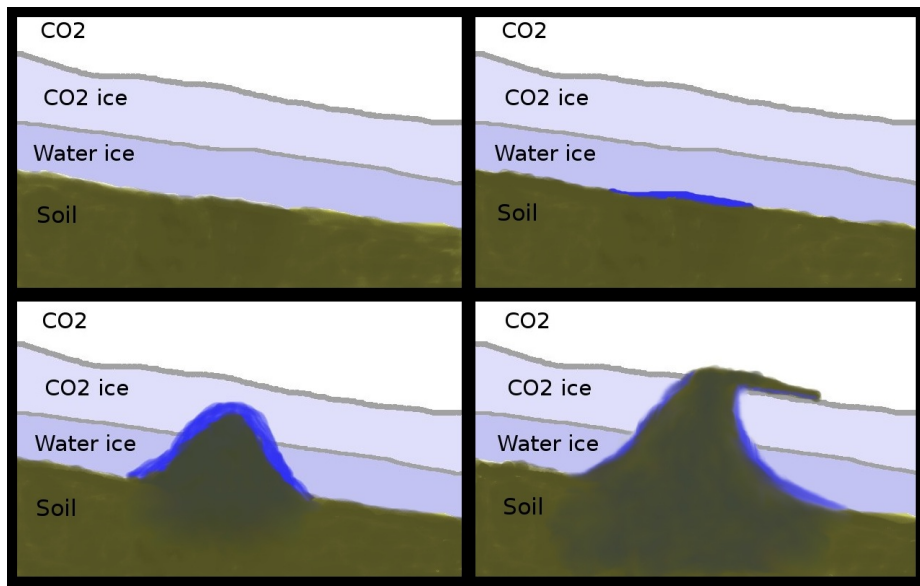


Figure 7.1: An illustration, made by Appel et al. (2010), of the step-by-step process of how a DDS emerges.

According to Appel et al. (2010), and illustrated in Figure 7.1 the ice eventually melts up to the surface, after creating a hole where the CO₂ ice layer is weak. When the soil-water mixture seeps out through the hole, it will carry some of the dark dune materials with it, and create the dark dune spot. Water in the soil-water mixture will eventually evaporate and the deposited soil will remain (Appel et al., 2010).

If the disappearance of DDSs next to dunes is due to high temperatures during Martian summer, then we should expect them to sustain in craters with dunes at high latitudes, above roughly 70°. This is, however, not the cause when observing Figure 6.8, showing only one crater, 72N_146E, following this claim. However, at quite low latitude, 65° N, the 65N_178E crater has DDSs visible next to dunes during the middle of the spring, at $L_s = 132^\circ$. This is a quite strange behavior, considering the theories stated above. The crater floor and the lower altitude atmosphere should experience a much higher temperature than those located at

higher latitude. It should be too warm for these spots to survive, so why are they there? Maybe the crater experienced a shock of cold air, freezing the crater temporarily at Martian Year 29.

7.6 Error sources

This work has analyzed images taken by the cameras CTX and HiRISE, riding on MRO. The CTX images are all taken in black and white. This has sometimes made it hard to distinguish the ice from the crater floor, within the crater. Most of the craters have a rugged crater floor, which sometimes reminds of layers or small plateaus that sometimes look almost the same as ice deposits. Also, the human eye is sometimes capable to see depths and hollowed out areas as something that is higher compared to the crater floor, and vice versa. This might lead to an incorrect description of the crater morphology.

On Mars NPR there are many impacts, and this work has only scratched a little on the surface. Almost 90 craters have been observed. Some of the craters have only two or less covering them. By only analyzing two images over different seasons, not much can be said of variation of the crater or the features within them. To follow up these craters more images are needed.

Chapter 8

Future Work

To understand and to observe changing in ice deposits and other features that have been observed within the craters, the work needs to be followed up in the future. Only over time will we be able to answer all the questions we have today. But also, in order to see or recognize different patterns around the northern hemisphere more craters need to be mapped. Only then, can we be more certain of how the ice changes. This work has analyzed almost 90 craters, which is only a small part of all the impacts on the northern hemisphere. Still there are craters with no images covering them. However, the crater impacts on the northern hemisphere are much fewer compared to the southern hemisphere. But in contrast to the southern hemisphere, the northern hemisphere is harder to observe due to the Martian orbit.

For future science of the Martian northern hemisphere, information of all images of the craters have been stored together with a small description, in a database. The database is not yet official but as the work continues to map all craters on the northern hemisphere, the database will be accessible. To make it easier for future work, the author will be working to put the database online on the NASA Ames homepage. The database will also be accessible on Adrian Brown's homepage: <http://abrown.seti.org/>.

Vocabulary

Acidalia Planitia A plain on Mars, located between the Tharsis volcanic province and the Arabia Terra, to the north of Valles Marineris

Alba Fossae Located in the Valles Marineris, 26° to 61° in latitude and 90° to 139° west in longitude

Chasma Boreale A large canyon located 83° latitude and 41° longitude on the Martian polar region

CRSIM Compact Reconnaissance Imaging Spectrometer for Mars

CTX ConTeXt Camera riding on MRO

DDS Dark spots appearing on Martian dunes

Deposition The opposite of sublimation, gas to solid

Dune Sand formation compared to those on the Earth

Dust Devils Black traces made by vortices

Evaporation The phase change going directly from liquid to gas

FAA Federal Aviation Administration

Gemina Lingula A plateau located south-east of Chasma Boreale

Gully A deep ditch supposed to have been created by running water

HiRISE High Resolution Imaging Science Experiment Camera, riding on MRO

LCROSS Lunar Crater Observations and Sensing Satellite

Mars Pathfinder Meteorological station

MGS Mars Global Surveyor

MRO Mars Reconnaissance Orbiter, satellite orbiting around Mars

NACA National Advisory Committee for Aeronautics

NASA National Aeronautics and Space Administration

Olympia Planitia A fan-shaped region located at 80° to 85° in latitude and at 140° to 240° in longitude

Polygonal nets A polygonal structure that can be seen on a crater floor

Scandia Colles An area with its center at 66.4° latitude and -137.20° longitude

SETI Search for Extra-Terrestrial Intelligence

Siton Undae A officially named dune field, located between 75°N and 82°N which spans about 200° in longitude

SOFIA Stratospheric Observatory for Infrared Astronomy

Solar longitude Martian time measure, where one degree in solar longitude corresponds to two Earth days

Sublimation The phase change going directly from solid/ice to gas

Tantalus Fossae An area with several large cracks, located at 50.9°N and 97.5°W

Vastitas Borealis Encircles the NPR as the largest lowland region on Mars

References

- Appel, M., Ramstad, R., Brown, A. J., McKay, C. P., and Fredriksson, S. (2010). Potential model for dark albedo features in the Martian polar region observed at 81°N 156°E. *LPSC XXXI*.
- Baerg, M., Beck, J., Hulme, S., Lievense, S., Tozzi, E., Bowman, C., Viotti, M., and Webster, G. (2010a). Mars Reconnaissance Orbiter: CRISM. <http://marsprogram.jpl.nasa.gov/mro/mission/instruments/crismcompactreconnaissanceimagingsspectrometerformars/>, Retrieved: March 10, 2010.
- Baerg, M., Beck, J., Hulme, S., Lievense, S., Tozzi, E., Bowman, C., Viotti, M., and Webster, G. (2010b). Mars Reconnaissance Orbiter: Instruments. <http://marsprogram.jpl.nasa.gov/mro/mission/instruments/>, Retrieved: March 10, 2010.
- Baerg, M., Beck, J., Hulme, S., Lievense, S., Tozzi, E., Bowman, C., Viotti, M., and Webster, G. (2010c). Mars Reconnaissance Orbiter: Overview. <http://marsprogram.jpl.nasa.gov/mro/mission/overview/>, Retrieved: March 10, 2010.
- Baerg, M., Beck, J., Hulme, S., Lievense, S., Tozzi, E., Bowman, C., Viotti, M., and Webster, G. (2010d). Odyssey: Multimedia. <http://mars.jpl.nasa.gov/gallery/sanddunes/>, Retrieved: February 12, 2010.
- Balme, M. and Greeley, R. (2006). Dust devils on Earth and Mars. *Rev. Geophys.*, 44:1–22.
- Beisser, K. (2010). Crism: Seeing the surface. <http://crism.jhuapl.edu/instrument/seeSurface.php>, Retrieved: March 10, 2010.
- Bennett, J., Shostak, S., and Jakosky, B. (2002). *Life in Universe*. Number 0-8053-8577-0. Pearson Education, Inc., publishing as Addison Wesley.
- Byrne, S. (2009). The Polar Deposits of Mars. *Annu. Rev. Earth Planet Sci.*, 37:535.
- Calvin, W. (2008). Summer season variability of the north residual cap of Mars as observed by the Mars Global Surveyor Thermal Emission Spectrometer (MGS-TES). *Planetary and Space Science*, 56:212.
- Dino, J. (2008). Ames Research Center Overview. <http://www.nasa.gov/centers/ames/about/overview.html>, Retrieved: February 5, 2010.
- Ferri, F., Smith, P. H., Lemmon, M., and Renno, N. O. (2003). Dust devils as observed by Mars Pathfinder. *J. Geophys. Res.*, 108.

-
- Grundy, W. M. and Schmitt, B. (1998). The temperature-dependent near-infrared absorption spectrum of hexagonal H₂O ice. *J. Geophys. Res.*, 103:802.
- Hale, A. S., Bass, D., and Tamppari, L. (2005). Monitoring the perennial Martian northern polar cap with MGS MOC. *Icarus*, 174:502.
- Hansen, G. B. (2005). Ultraviolet to near-infrared absorption spectrum of carbon dioxide ice from 0.174 to 1.8 μ . *J. Geophys. Res.*, 110.
- Ingersoll, A. P., Svitek, T., and Murray, B. C. (1992). Stability of polar frosts in spherical bowl-shaped craters on the Moon, Mercury, and Mars. *Icarus*, 100:40.
- Jakosky, B. M. and Haberle, R. M. (1992). *Mars: The seasonal behaviour of water on Mars*. Number 978-0816512577. The University of Arizona Press.
- James, P., Hansen, G., and Titus, T. (2005). The carbon dioxide cycle. *Advances in Space Research*, 35:14.
- Malin, M. C., III, J. F. B., Cantor, B. A., and Caplinger, M. A. (2007). Context Camera Investigation on board the Mars Reconnaissance Orbiter. *J. Geophys. Res.*, 112.
- Mangimeli, J. (2010). Geology of sand dunes. <http://www.nps.gov/archive/whsa/Sand%20Dune%20Geology.htm>, Retrieved: February 12, 2010.
- McEwen, A. S., Eliason, E. M., Bergstrom, J. W., and Bridges, N. T. (2007). Mars Reconnaissance Orbiter's High Resolution Imaging Science Experiment (HiRISE). *J. Geophys. Res.*, 112.
- Murchie, S., Arvidson, R., Bedini, P., Beisser, K., and Bishop, J. (2007). Compact Reconnaissance Imaging Spectrometer for Mars (CRISM) south polar mapping: First Mars year of observations. *J. Geophys. Res.*, 112.
- Renno, N. O., Nash, A. A., Lunine, J., and Murphy, J. (2000). Martian and terrestrial dust devils: Test of a scaling theory using Pathfinder. *J. Geophys. Res.*, 105:1859.
- Russell, R. (2009). Carbon Dioxide. http://www.windows.ucar.edu/tour/link=/physical_science/chemistry/carbon_dioxide.html&cdp=/windows3&edu=high, Retrieved: March 24, 2010.
- SETI (2010a). The Center for SETI Research. <http://www.seti.org/seti>, Retrieved: February 8, 2010.
- SETI (2010b). History of SETI. <http://www.seti.org/Page.aspx?pid=572>, Retrieved: February 8, 2010.
- SETI (2010c). Our mission. <http://www.seti.org/about-us/>, Retrieved: February 8, 2010.
- Smith, D. E., Zuber, M. T., Frey, H. V., Garvin, J. B., Head, J. W., Muhleman, D. O., Pettengill, G. H., Phillips, R. J., Solomon, S. C., Zwally, H. J., Banerdt, W. B., and Duxbury, T. C. (1998). Shape of the northern hemisphere of Mars from the Mars Orbiter Laser Altimeter (MOLA). *Science*, 279:1686.
- Steven, W. (2004). Mars. http://www.nasa.gov/worldbook/mars_worldbook.html, Retrieved: February 5, 2010.

REFERENCES

- Suckow, E. (2009). Overview. <http://history.nasa.gov/naca/overview.html>, Retrieved: February 5, 2010.
- Tanaka, K. L. and Scott, D. H. (1987). Geologic map of the polar regions on Mars. *U.S. Department of the Interior, U.S. Geological Survey*, page 10.
- Titus, T. N., Calvin, W. M., Kieffer, H., Langevin, Y., and Prettyman, T. H. (2008). *Martian polar processes*. Number 978-0-511-41372-8. Cambridge University Press, Cambridge.
- Weselby, C. (2009). Hangar One Overview. http://www.nasa.gov/centers/ames/home/2008/hangar_index.html, Retrieved: February 5, 2010.
- Xie, H., Guan, H., Zhu, M., and Thueson, M. (2007). A Conceptual Model of H₂O/CO₂ Frost Sublimation and Condensation Caused Albedo Change in Crater Interiors, Martian Seasonal Polar Cap Regions. *LPSC*, XXXVIII.

Bibliography

Armstrong, J., Nielson, S. and Titus, T. (2007), Survey of TES high albedo events in Mars' northern craters, *Geophys. Res. Lett.*, 34, 1-4.

Bland, P. A., McBride, N., Moore, E. A., Widdowson, M. Wright, I. McBride, N. and, Lain Gilmore (eds.) (2004), An Introduction to the Solar System, *The Open University, Cambridge University Press*, 145.

Garvin, J. B., Sakimoto, S. E., Frawley, J. J. and Schnetzler, C. (2000), North Polar Region Craterforms on Mars: Geometric Characteristics from the Mars Orbiter Laser Altimeter, *Icarus*, 144, 329.

Kieffer, H. H. and Titus, T. N. (2001), TES Mapping of Mars' North Seasonal Cap, *Icarus*, 154, 162.

Xie, H., Guan, H., Zhu, M., Thueson, M., Ackley, S. and, Yue, Z. (2008), A conceptual model for explanation of Albedo changes in Martian craters, *Planetary and Space Science*, 56, 887.

Appendix

On the following pages, all images for each crater are listed with their official image ID and the corresponding camera.

Images taken by the CTX camera can be found with their specific image ID, on the following home page:

<http://viewer.mars.asu.edu/planetview/inst/ctx/#start>

Images taken by the HiRISE camera can be found with their specific image ID, on the following home page:

<http://hirise.lpl.arizona.edu/anazitisi.php>

Unnamed craters in latitudinal order

Crater name:	60N_148E	P21_009269_2409_XN_60N270W
CTX images:	P18_008054_2407_XN_60N212W	P20_008768_2408_XN_60N270W
HiRISE image:	PSP_008054_2405	P22_009836_2408_XN_60N270W
		B02_010403_2408_XN_60N270W
Crater name:	60N_129E	HiRISE images:
CTX images:	P17_007646_2406_XN_60N230W	PSP_007832_2410
	P18_008081_2406_XN_60N230W	
	P20_008727_2406_XN_60N230W	Crater name:
	P20_008793_2406_XN_60N230W	61N_88E
	B02_010362_2406_XN_60N230W	CTX images:
		P16_007397_2409_XN_60N272W
		P17_007542_2409_XN_60N272W
		B02_010535_2409_XN_60N272W
		P19_008336_2422_XN_62N353W
Crater name:	60N_101E	
CTX images:	P16_007193_2409_XN_60N102W	Crater name:
	P19_008340_2409_XN_60N101W	61N_229E
HiRISE image:	PSP_010054_2410	CTX images:
		P19_008341_2420_XN_62N131W
Crater name:	60N_222E	
CTX images:	P15_006957_2405_XN_60N138W	Crater name:
	P17_007603_2405_XN_60N138W	61N_22E
	P18_008104_2424_XN_62N138W	CTX images:
HiRISE image:	PSP_008104_2405	P17_007729_2417_XN_61N338W
		P19_008375_2418_XN_61N338W
Crater name:	60N_313E	
CTX images:	P17_007626_2418_XN_61N047W	Crater name:
	P18_008127_2407_XN_60N046W	61N_312E
	P21_009274_2407_XN_60N046W	CTX images:
		P17_007547_2429_XN_62N049W
		P18_008193_2416_XN_61N048W
		HiRISE image:
		PSP_007547_2415
Crater name:	60N_281E	
CTX images:	P17_007825_2405_XN_60N079W	Crater name:
	P18_008181_2405_XN_60N079W	61N_308E
	P19_008326_2405_XN_60N079W	CTX images:
HiRISE image:	PSP_008181_2405	P15_006967_2418_XN_61N051W
	PSP_010396_2405	P17_007613_2424_XN_62N052W
		HiRISE image:
		PSP_006967_2420
		PSP_007613_2420
Crater name:	60N_251E	
CTX images:	P18_008037_2405_XN_60N109W	Crater name:
		62N_6E
		CTX images:
		P19_008336_2422_XN_62N353W
		P17_007545_2422_XN_62N354W
		P17_007690_2422_XN_62N353W
Crater name:	61N_90E	
CTX images:	P16_007186_2400_XN_60N270W	Crater name:
	P17_007832_2408_XI_60N270W	62N_222E
	P18_008122_2400_XN_60N270W	CTX images:
	P19_008333_2409_XN_60N272W	P18_008104_2424_XN_62N138W
	P21_009335_2409_XN_60N272W	P18_008249_2429_XN_62N138W
		Crater name:
		63N_12E
		CTX images:
		P16_007202_2440_XN_64N348W
		P17_007558_2439_XN_63N349W
		HiRISE images:
		PSP_008204_2440

Crater name:	63N_187E		P18_008100_2462_XN_66N030W
CTX images:	P02_001908_2431_XI_63N173W		B02_010236_2459_XN_65N030W
	P17_007512_2432_XN_63N173W	HiRISE image:	PSP_008456_2460
	P17_007657_2432_XN_63N172W		PSP_010236_2460
	P18_008013_2431_XN_63N173W		
	P18_008158_2431_XN_63N173W	Crater name:	65N_339E
HiRISE image:	PSP_001908_2430	CTX images:	P16_007335_2448_XN_64N020W
	PSP_009806_2430		P17_007691_2446_XN_64N021W
	PSP_010228_2430		B02_010473_2458_XN_65N021W
	PSP_010439_2430		
Crater name:	63N_292E	Crater name:	65N_210E
CTX images:	T01_000875_2440_XI_64N067W	CTX images:	P16_007142_2449_XN_64N152W
	P16_007429_2440_XN_64N067W		P17_007788_2450_XN_65N150W
	P18_008141_2440_XN_64N067W	Crater name:	65N_178E
HiRISE image:	PSP_007429_2440	CTX images:	P03_002027_2453_XI_65N182W
	PSP_007574_2440		P13_006207_2454_XN_65N181W
	PSP_007640_2440		P17_007565_2453_XN_65N182W
	PSP_008141_2440		P17_007710_2455_XN_65N180W
Crater name:	63N_296E		P18_008066_2453_XN_65N182W
	P15_007007_2440_XN_64N064W	HiRISE images:	B01_010136_2453_XN_65N182W
	P17_007508_2440_XN_64N064W		PSP_002027_2455
	P18_008154_2440_XN_64N064W		PSP_010136_2455
HiRISE image:	PSP_007508_2440		PSP_010413_2455
Crater name:	64N_132E	Crater name:	65N_128E
CTX images:	P15_007013_2437_XN_63N228W	CTX images:	P16_007435_2452_XN_65N231W
	P17_007659_2438_XN_63N228W		P17_007580_2473_XN_67N231W
HiRISE images:	PSP_007659_2440		P18_007936_2456_XN_65N232W
Crater name:	64N_31E		P18_008147_2456_XN_65N231W
CTX images:	P17_007755_2451_XN_65N329W		P20_008661_2456_XN_65N231W
Crater name:	64N_234E		B02_010507_2456_XN_65N231W
CTX images:	P17_007563_2446_XN_64N126W	Crater name:	66E_144E
Crater name:	65N_284E	CTX images:	P15_006762_2466_XN_66N215W
CTX images:	P15_006836_2457_XN_65N076W		P15_006973_2465_XN_66N216W
	P17_007627_2469_XN_66N076W	HiRISE image:	P18_008120_2477_XN_67N216W
	P17_007693_2455_XN_65N076W		PSP_008120_2465
HiRISE image:	PSP_010053_2455	Crater name:	66N_40E
Crater name:	65N_330E	CTX images:	P16_007135_2465_XN_66N320W
CTX images:	P15_006953_2462_XN_66N030W		P17_007491_2465_XN_66N321W
	P03_002417_2456_XI_65N030W		P17_007636_2465_XN_66N320W
	P15_006953_2462_XN_66N030W		P17_007781_2465_XN_66N320W
			P18_008071_2465_XN_66N320W

Crater name:	66N_163E		P18_008171_2486_XN_68N170W
CTX images:	P15_007025_2465_XN_66N196W	HiRISE image:	PSP_010241_2485
	P18_008119_2420_XN_62N189W		
	P18_008238_2465_XN_66N196W	Crater name:	68N_13E
	P20_008752_2466_XN_66N196W	CTX images:	P17_007571_2487_XN_68N347W
HiRISE image:	PSP_008172_2465		P18_008072_2487_XN_68N347W
			P20_008718_2486_XN_68N347W
			B02_010353_2487_XN_68N347W
Crater name:	67N_250E	HiRISE images:	PSP_007571_2490
CTX images:	P16_007180_2474_XN_67N111W		
	P18_008037_2474_XN_67N111W	Crater name:	69N_26E
	P18_008182_2474_XN_67N110W	CTX images:	P16_007175_2492_XN_69N332W
			P18_008177_2491_XN_69N333W
Crater name:	67N_114E		P20_008757_2491_XN_69N333W
CTX images:	P16_007185_2473_XN_67N246W	HiRISE images:	PSP_008757_2490
	P17_007541_2478_XN_67N247W		
	P18_008253_2473_XN_67N246W	Crater name:	69N_41E
	P20_008912_2473_XN_67N246W	CTX images:	P16_007214_2496_XN_69N318W
	P22_009545_2472_XN_67N246W		P19_008361_2496_XN_69N318W
HiRISE images:	PSP_008912_2470		
		Crater name:	70N_285E
Crater name:	67N_98E	CTX images:	P17_007561_2500_XN_70N075W
CTX images:	P16_007212_2472_XN_67N263W		P19_008273_2500_XN_70N075W
	P16_007357_2472_XN_67N262W	HiRISE image:	PSP_008352_2500
	P17_007502_2472_XN_67N261W		
		Crater name:	70N_13E
Crater name:	67N_93E	CTX images:	P17_007650_2503_XN_70N346W
CTX images:	P15_006988_2480_XN_68N267W		P18_008151_2502_XN_70N346W
	P17_007489_2480_XN_68N267W	HiRISE images:	PSP_007650_2505
	P17_007786_2919_XN_68N267W		
	P19_008346_2481_XN_68N267W	Crater name:	70N_352E
	P21_009348_2481_XN_68N267W	CTX images:	P13_006161_2502_XI_70N007W
	B01_009915_2481_XN_68N267W		P15_007084_2501_XN_70N009W
HiRISE image:	PSP_009915_2480		P16_007229_2530_XN_73N009W
			P16_007374_2502_XN_70N007W
Crater name:	67N_252E		P17_007519_2502_XN_70N007W
CTX images:	P18_008116_2474_XN_67N108W		P18_008165_2502_XN_70N008W
HiRISE image:	PSP_007615_2470		P19_008310_2502_XN_70N008W
			P22_009457_2502_XN_70N008W
Crater name:	67N_223E	HiRISE image:	PSP_008165_2505
CTX images:	P16_007392_2479_XN_67N138W		PSP_009457_2505
	P17_007682_2479_XN_67N137W		PSP_009734_2505
	P19_008328_2480_XN_68N137W		PSP_010512_2505
			PSP_010868_2505
Crater name:	68N_190E		
CTX images:	P16_007380_2486_XN_68N170W		
	P17_007525_2486_XN_68N170W		
	P18_008026_2486_XN_68N170W		

Crater name:	70N_267E		P19_008335_2532_XN_73N332W
CTX images:	P04_002617_2505_XI_70N092W		
	P16_007153_2505_XN_70N093W	Crater name:	73N_178E
	P16_007364_2505_XN_70N095W	CTX images:	P17_007499_2535_XN_73N181W
	P17_007799_2513_XN_71N093W		P18_008079_2536_XN_73N181W
HiRISE image:	PSP_007153_2505		P18_008145_2536_XN_73N181W
	PSP_007799_2505	HiRISE images:	PSP_007499_2535
	PSP_009803_2505		
	PSP_009935_2505	Crater name:	74N_187E
Crater name:	71N_194E	CTX images:	P16_007380_2540_XN_74N173W
CTX images:	P15_007037_2509_XN_70N166W		P17_007670_2541_XN_74N172W
	P16_007182_2513_XN_71N165W		P17_007736_2540_XN_74N174W
	P16_007393_2508_XN_70N167W		P19_008382_2540_XN_74N173W
	P17_007683_2513_XN_71N166W	Crater name:	74N_347E
	P18_008184_2510_XN_71N166W	CTX images:	P16_007150_2543_XN_74N013W
HiRISE image:	PSP_006892_2510		P18_007941_2543_XN_74N012W
			P18_008086_2544_XN_74N012W
Crater name:	72N_146E		
CTX images:	P17_007566_2523_XN_72N214W	Crater name:	74N_13E
	P18_008133_2522_XN_72N214W	CTX images:	P13_006292_2569_XN_76N349W
HiRISE images:	PSP_010203_2525		P17_007584_2549_XN_74N346W
		HiRISE images:	PSP_007584_2550
Crater name:	72N_144E		
CTX images:	P16_007197_2524_XN_72N215W	Crater name:	74N_319E
	P17_007698_2526_XN_72N216W	CTX images:	P15_006795_2544_XN_74N040W
	P18_008199_2526_XN_72N215W		P16_007151_2552_XN_75N041W
	P20_008845_2526_XN_72N215W		P17_007507_2543_XN_74N040W
	P21_009346_2526_XN_72N215W		P18_008153_2544_XN_74N040W
			P19_008443_2544_XN_74N040W
Crater name:	72N_345E		
CTX images:	P17_007572_2520_XN_72N015W	Crater name:	75N_15E
	P18_008073_2520_XN_72N015W	CTX images:	P17_007729_2557_XN_75N344W
HiRISE image:	PSP_007572_2520		P18_008164_2553_XN_75N345W
	PSP_010077_2520		P21_009087_2550_XN_75N345W
		HiRISE images:	PSP_009087_2550
Crater name:	73N_2E		
CTX images:	P15_006833_2537_XN_73N357W	Crater name:	75N_340E
	P19_008270_2537_XN_73N357W	CTX images:	P15_006992_2551_XN_75N020W
HiRISE images:	PSP_006833_2540		P20_008713_2848_XN_75N019W
Crater name:	73N_22E		
CTX images:	P17_007597_2532_XN_73N338W	Crater name:	75N_158E
HiRISE images:	PSP_007597_2530	CTX images:	P17_007592_2564_XN_76N202W
			P17_007526_2556_XN_75N201W
Crater name:	73N_27E		P20_008667_2844_XN_75N201W
CTX images:	P17_007755_2531_XN_73N333W		B02_010308_2568_XI_76N202W

Crater name:	76N_159E		P22_009726_2833_XN_76N313W
CTX images:	P17_007526_2556_XN_75N201W P17_007592_2564_XN_76N202W B02_010308_2568_XI_76N202W	Crater name:	78N_52E
		CTX images:	T01_000857_2581_XI_78N307W P13_006264_2574_XN_77N305W P16_007187_2581_XN_78N307W P18_008110_2581_XN_78N307W
Crater name:	76N_333E		
CTX images:	P16_007335_2564_XN_76N026W P17_007691_2564_XN_76N027W P18_008126_2564_XN_76N027W	Crater name:	78N_41E
		CTX images:	P02_001702_2572_XN_77N318W P13_006225_2581_XN_78N321W P17_007728_2581_XN_78N320W
Crater name:	77N_196E		
CTX images:	P16_007195_2577_XN_77N165W P17_007696_2568_XN_76N165W P18_008178_2829_XN_77N164W B01_009977_2580_XI_78N166W	HiRISE image:	P18_008163_2581_XN_78N320W PSP_007583_2580
Crater name:	77N_90E	Crater name:	78N_346E
CTX images:	P02_001687_2575_XN_77N269W P02_001819_2570_XN_77N270W P13_006144_2577_XN_77N269W P13_006210_2576_XN_77N271W P14_006566_2568_XN_76N270W P15_006711_2568_XI_76N270W P15_006777_2569_XI_76N270W P15_006922_2569_XN_76N270W P16_007133_2566_XI_76N270W P16_007259_2832_XN_76N271W P17_007568_2567_XI_76N270W P18_007924_2551_XN_75N269W P18_008069_2569_XN_76N270W P19_008359_2567_XI_76N270W P19_008551_2832_XI_76N270W P19_008570_2567_XI_76N270W P20_008715_2567_XN_76N271W P20_008860_2566_XI_76N270W P20_008939_2572_XN_77N270W P22_009638_2573_XN_77N272W	CTX images:	P01_001506_2600_XN_80N015W P16_007374_2595_XN_79N015W P17_007664_2585_XN_78N012W
		Crater name:	79N_62E
		CTX images:	P02_001688_2617_XI_81N303W P13_006145_2572_XN_77N296W P13_006211_2582_XN_78N299W P13_006290_2583_XN_78N296W P14_006501_2583_XN_78N297W P15_006857_2592_XN_79N299W P18_008183_2808_XN_79N299W P20_008795_2592_XN_79N299W P22_009507_2586_XN_78N298W B02_010496_2592_XN_79N299W
HiRISE images:	PSP_007779_2570 PSP_008926_2575	HiRISE images:	PSP_008426_2595
Crater name:	77N_46E	Crater name:	79N_240E
CTX images:	P13_006172_2582_XN_78N314W P13_006238_2573_XN_77N315W P17_007596_2568_XN_76N313W P18_008031_2567_XN_76N313W	CTX images:	P13_006178_2578_XN_77N118W P17_007602_2582_XN_78N120W P18_008103_2582_XN_78N120W PSP_008103_2580
		Crater name:	81N_117E
		CTX images:	T01_000894_2622_XN_82N243W P18_008168_2786_XN_81N242W

Named craters in alphabetic order

Crater name:	Boola Crater	P15_006979_2587_XN_78N028W
CTX images:	P17_007667_2614_XN_81N105W	P17_007625_2599_XN_79N030W
	P18_008097_2787_XN_81N105W	P18_008028_2813_XN_78N028W
	P01_001496_2603_XN_80N103W	P20_008693_2587_XN_78N028W
		P21_009062_2597_XN_79N029W
Crater name:	Crotone Crater	B02_010407_2587_XN_78N028W
CTX images:	P17_007837_2611_XI_81N064W	HiRISE image: TRA_000860_2585
	P18_007903_2611_XN_81N066W	PSP_008416_2585
	P02_001653_2623_XN_82N070W	
HiRISE image:	PSP_009986_2625	
Crater name:	Dokka Crater	Crater name: Jojutla Crater
CTX images:	P13_006179_2582_XN_78N145W	CTX images: P01_001427_2787_XI_81N170W
	P13_006245_2587_XN_78N148W	P02_001723_2610_XN_81N176W
	P15_006746_2572_XN_77N145W	P18_007941_2785_XN_81N167W
	P17_007682_2573_XN_77N143W	P18_008065_2616_XN_81N170W
	P17_007748_2563_XN_76N144W	P18_008131_2616_XN_81N169W
		P20_008877_2784_XN_81N169W
		P21_009299_2784_XN_81N169W
Crater name:	Escorial Crater	TRA_000865_2615
CTX images:	P13_006189_2558_XN_75N056W	PSP_008131_2615
	P13_006202_2559_XN_75N051W	
	P15_006980_2590_XN_79N056W	Crater name: Korolev Crater
	P16_007191_2561_XN_76N054W	CTX images: P01_001592_2530_XI_73N195W
	P20_008773_2570_XN_77N054W	P03_002291_2530_XN_73N193W
		P13_006181_2527_XN_72N195W
Crater name:	Heimdall Crater	P15_006959_2528_XN_72N196W
CTX images:	P16_007431_2482_XI_68N124W	P15_007038_2530_XN_73N194W
	P17_007787_2481_XI_68N125W	P16_007473_2538_XN_73N193W
	P18_008077_2482_XI_68N124W	P17_007816_2528_XN_72N198W
	P19_008433_2484_XI_68N124W	P18_007961_2529_XN_72N197W
	P21_009079_2485_XI_68N124W	P20_008765_2530_XN_73N193W
	P21_009092_2484_XI_68N124W	P20_008831_2529_XN_72N195W
	P21_009435_2484_XN_68N125W	P20_008963_2529_XI_72N195W
	P22_009580_2485_XI_68N124W	P21_009042_2528_XI_72N197W
	P22_009646_2484_XI_68N125W	P21_009332_2529_XN_72N194W
HiRISE image:	PSP_009580_2485	P22_009477_2530_XN_73N193W
	PSP_009778_2485	P22_009754_2529_XN_72N195W
	PSP_010299_2915	B02_010387_2529_XN_72N195W
	PSP_010358_2485	HiRISE images: PSP_001592_2530
	PSP_010714_2485	PSP_007961_2530
		PSP_010387_2530
Crater name:	Inuvik Crater	
CTX images:	P02_001665_2596_XN_79N031W	

Crater name:	Kunowsky Crater	PSP_007805_2505
CTX images:	P03_002179_2371_XI_57N009W	PSP_007950_2505
	P10_005080_2370_XN_57N010W	PSP_008095_2500
	P11_005225_2371_XN_57N008W	PSP_008161_2505
	P13_006214_2368_XN_56N010W	PSP_008240_2500
	P15_006860_2371_XN_57N009W	PSP_008530_2505
HiRISE image:	PSP_002179_2375	PSP_008741_2505
	PSP_006860_2370	PSP_008886_2505
	PSP_009721_2370	PSP_008952_2500
		PSP_009031_2505
Crater name:	Lomonosov Crater	PSP_009242_2505
CTX images:	P03_002047_2451_XI_65N008W	PSP_009453_2500
	P13_006227_2449_XN_64N007W	PSP_010587_2500
	P15_007005_2452_XN_65N010W	
	P16_007440_2450_XN_65N008W	Crater name:
	P17_007585_2450_XN_65N007W	Puyo Crater
	P17_007651_2452_XN_65N009W	CTX images:
	P17_007730_2454_XN_65N006W	B01_010203_2601_XN_80N221W
	P19_008297_2451_XN_65N009W	
	B01_009866_2451_XN_65N009W	Crater name:
HiRISE image:	PSP_007440_2455	Sevel Crater
	PSP_010011_2460	CTX images:
	PSP_010644_2455	P18_007889_2603_XN_80N039W
		P21_009115_2606_XN_80N036W
		P22_009537_2612_XI_81N039W
Crater name:	Lonar Crater	
CTX images:	P02_001966_2531_XI_73N321W	Crater name:
	P17_007715_2532_XN_73N321W	Udzha Crater
	P22_009719_2531_XI_73N321W	CTX images:
	P22_009798_2530_XI_73N321W	T01_000803_2620_XN_82N280W
HiRISE images:	PSP_001966_2530	P17_007563_2779_XN_82N283W
	PSP_007715_2530	P17_007700_2602_XN_80N279W
		P20_008992_2618_XI_81N282W
Crater name:	Louth Crater	
CTX images:	P01_001370_2503_XI_70N257W	
	P02_001700_2506_XI_70N256W	
	P15_006737_2504_XI_70N256W	
	P15_006803_2505_XN_70N257W	
	P17_007805_2504_XN_70N256W	
	P20_008965_2504_XN_70N255W	
HiRISE images:	PSP_001370_2505	
	PSP_001700_2505	
	PSP_006737_2505	
	PSP_006869_2505	
	PSP_007159_2505	
	PSP_007449_2505	
	PSP_007515_2500	
	PSP_007739_2505	

Attachment

On the following pages is an abstract for the Lunar Planetary Science Conference 2010. It describes the seasonal change of ice and other features, in Korolev crater, during the summer months.

MONITORING THE KOROLEV CRATER ON SPRING AND SUMMER IMAGES IN THE MARTIAN NORTHERN POLAR REGION WITH CTX AND HIRISE. S. A. M. Bertilsson¹, M. Hajigholi¹, A. J. Brown³, C. P. McKay⁴, S. Fredriksson¹. ¹Department of Physics, Luleå University of Technology, SE-971 87 Luleå, Sweden, ³SETI Institute, Mountain View, CA94043, ⁴NASA Ames, Moffett Field, CA94035. Email: angelique.bertilsson@gmail.com

Introduction: Change in albedo during spring and summer of the water ice covered crater Korolev have been previously reported. According to Armstrong et al. [1] Korolev exhibits an increase in summer time albedo, which they linked to water ice condensing during the summer months. Analyzing images of Korolev crater from different solar longitude, L_s , during spring and summer can help us understand how water behaves in the Martian Northern Polar Region, NPR. This work will analyze the images from CTX and HiRISE to map water ice and seasonal change in Korolev crater during northern spring and summer.

Location: Korolev crater is one of the northern Martian lowlands largest craters, roughly circular with an ~80 km diameter, containing significant ice rich material [2]. Figure 1 shows the location of Korolev crater relative to the residual cap at 73°N 165°E.

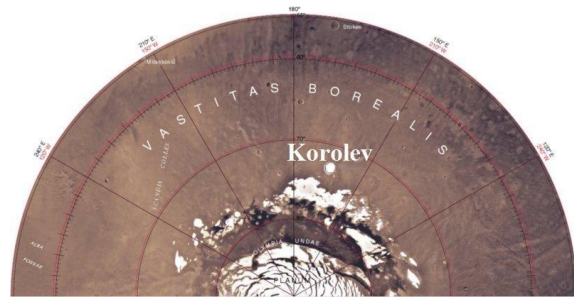


Figure 1. Topography map of Martian northern polar cap showing the location of Korolev crater at 73°N 165°E. Source: Viking Color Image.

HiRISE and CTX: HiRISE, High Resolution Imaging Science Experiment, is a high resolution camera riding on MRO. It commenced operations in 2006 and is a 0.5 m reflecting telescope which give a colored (red, green and IR) and detailed resolution of 0.25 meter per pixel [3]. CTX is a context camera designed to obtain grayscale images with a resolution of 6 meter per pixel and a swath width of 30 km [4].

Korolev Data: With help of Google Mars, we have identified eight CTX images and three HiRISE images covering Korolev from northern spring to summer. We have created a database (*Information on craters in the Martian Northern Polar Region*) [5], to store information about craters from the Martian northern polar region. When selecting the images of Korolev crater the following criteria have been utilized. The images of the crater should be over different seasons,

spring and summer, ordered by L_s . The crater should be clearly visible in all studied images and easily identified, i.e. no clouds or dust storms obscuring the crater. For information about Korolev crater all year around the reader is referred to M. Hajigholi et al. [5].

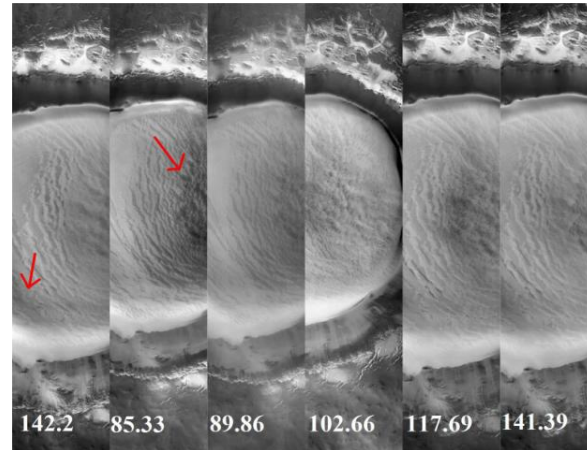


Figure 2. Korolev crater at different solar longitudes, L_s . Showing (left to right) how the albedo of the surface changes with time. P01_001592_2530_XI_73N195W, Martian Year 28, P20_008831_2529_XN_72N195W, Martian Year 29, P20_008963_2529_XI_72N195W, Martian Year 29, P21_009332_2529_XN_72N194W, Martian Year 29,

Analysis: In Figure 2 images of Korolev crater are ordered in solar longitude from $L_s=142.2^\circ$, northern summer in Martian Year (MY) 28 to $L_s=141.4^\circ$, northern summer, MY 29. The images are taken by CTX and show how a darker color from the left bottom and middle right corners change with time over the crater. Figure 3 shows four zoomed in images at the same area in the middle of the crater, from Figure 2, $L_s=142.2^\circ$ in MY 28, $L_s=85.33^\circ$ in MY 29, $L_s=89.86^\circ$ in MY 29 and $L_s=141.4^\circ$ in MY 29. We have observed dark lineated features covering the icy surface in spring which later disappear in the summer. This behavior may be related to the albedo changes observed by Armstrong et al. [6].

Figures 4 – 8 show images from CTX and HiRISE (from top to bottom) located at 73°N 165°E, taken at the same solar longitude, $L_s=142.2^\circ$ in MY 28. Figure 5, a HiRISE image, shows how the surface in the middle of the crater has smooth rippled terrain with darker lines of roughened terrain [7]. This could be due to a surface with a mixture of different material and layers with an icy regolith underneath. According to

Armstrong [6] a thermal pulse traveling through the regolith is capable of releasing water vapor from the icy regolith. This water vapor can then supply as a local reservoir that can condense in mid summer.

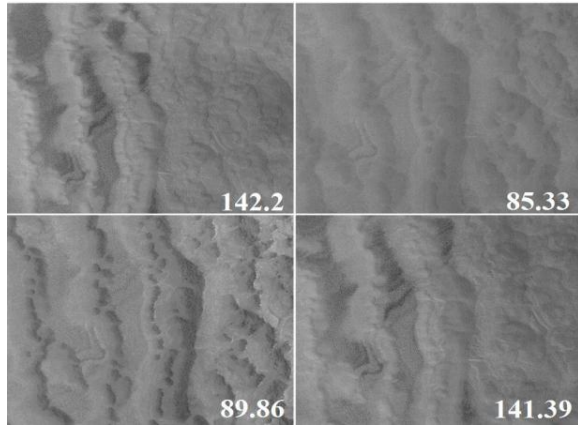


Figure 3. Images zoomed in to the same region in the middle of the crater ordered by L_s . Left to right top images: P01_001592_2530_XI_73N195W, MY 28, P20_008831_2529_XN_72N195W, MY 29, Left to Right bottom images: P20_008963_2529_XI_72N195W, MY 29, B02_010387_2529_XN_72N195W, MY 29

The higher albedo of ice allows the light to penetrate ice relatively easily. Depending on what might be underneath the high albedo surface, the sub-surface will absorb the sunlight and cause the covered material to heat up. This “solid state greenhouse” effect will eventually cause the overlying water ice to vaporize (from below) but if this process is incomplete it might temporarily leave behind a “remnant material”. Depending on what kind of material could be stored under the ice, the surface may have a lower albedo, creating the darker lines seen on the CTX and HiRISE images, Figures 4 – 8. To find out if these black lines might change the color of the surface over time, images from the same solar longitude but in MY 29, have been studied from CTX and HiRISE. Unfortunately the images taken by HiRISE do not show this area of the crater and the theory can therefor not be confirmed. Looking at CTX images from spring at the same solar longitude as above, the black lines can be seen. This might indicate that the black lines are not responsible for how the surface albedo changes. If the change of the crater surface depends on solar longitude, a daily variation or due to temperature changing within the crater remains to be solved.

Conclusions: By monitoring and analyzing the images of craters in the Martian northern polar region, especially ice covered craters like Korolev, a deeper understanding of how water behaves on the Martian northern polar cap and what kind of influence it has on the CO_2 cycle between the northern and southern he-

misphere can be reached. To understand what might cause the change of the surface albedo in Korolev, more images has to be taken in high resolution with HiRISE over different seasons to monitor the change over time and what relation the change might have due to temperature when comparing high resolution images with Thermal Emission Spectrum, TES, observations and thermal models.

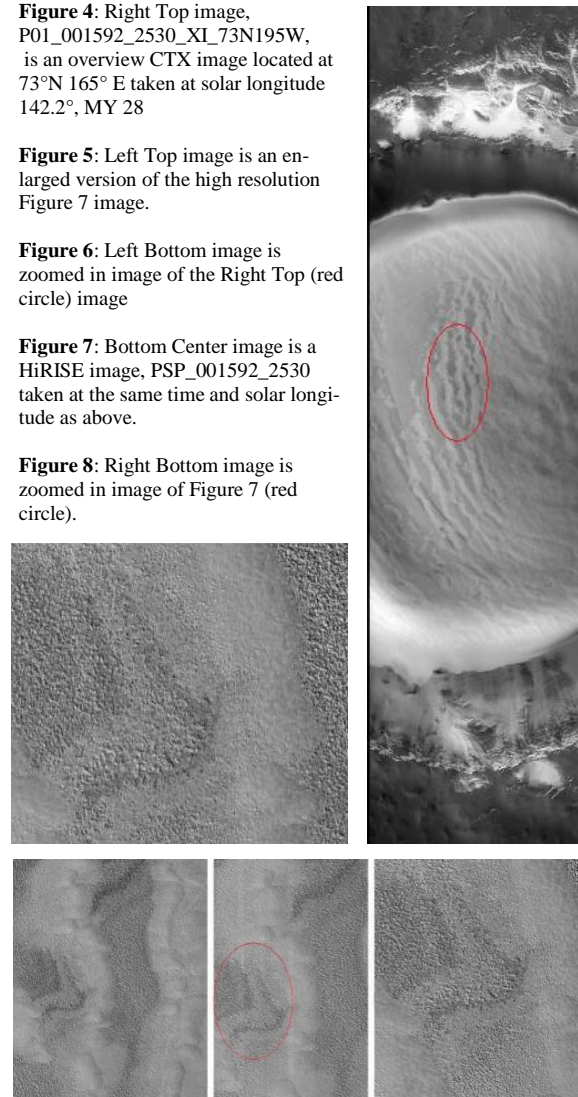
Figure 4: Right Top image, P01_001592_2530_XI_73N195W, is an overview CTX image located at $73^\circ\text{N } 165^\circ\text{E}$ taken at solar longitude 142.2° , MY 28

Figure 5: Left Top image is an enlarged version of the high resolution Figure 7 image.

Figure 6: Left Bottom image is zoomed in image of the Right Top (red circle) image

Figure 7: Bottom Center image is a HiRISE image, PSP_001592_2530 taken at the same time and solar longitude as above.

Figure 8: Right Bottom image is zoomed in image of Figure 7 (red circle).



- References:** [1] Armstrong J. C. et al. (2004) *LPS XXXV* Abstract #1744. [2] Russell P. S. et al. (2004) *LPS XXXV* Abstract #2007. [3] McEwen A. S. et al. (2007), *JGR*, 112, doi:10.1029/2005JE00265. [4] Malin M. C. et al. (2007), *JGR*, 112, doi:10.1029/2006JE002808. [5] Hajigholi M. et al. (2009), *LPSC XXXXI*, this meeting. [6] Armstrong, J.C. and Titus, T.N. (2005) *Icarus* 174, 360–372. [7] Brown A. J. et al. (2007) *LPS XXXXI*, Abstract #2262.